

---

# Simplex-enabled Safe Continual Learning Machine

---

Anonymous Author(s)

Affiliation

Address

email

## Abstract

This paper proposes the **SeC-Learning Machine**: Simplex-enabled safe continual learning for safety-critical autonomous systems. The SeC-learning machine is built on Simplex logic (that is, “using simplicity to control complexity”) and physics-regulated deep reinforcement learning (Phy-DRL). The SeC-learning machine thus constitutes HP (high performance)-Student, HA (high assurance)-Teacher, and Coordinator. Specifically, the HP-Student is a pre-trained high-performance but not fully verified Phy-DRL, continuing to learn in a real plant to tune the action policy to be safe. In contrast, the HA-Teacher is a mission-reduced, physics-model-based, and verified design. As a complementary, HA-Teacher has two missions: backing up safety and correcting unsafe learning. The Coordinator triggers the interaction and the switch between HP-Student and HA-Teacher. Powered by the three interactive components, the SeC-learning machine can i) assure lifetime safety (i.e., safety guarantee in any continual-learning stage, regardless of HP-Student’s success or convergence), ii) address the Sim2Real gap, and iii) learn to tolerate unknown unknowns in real plants. The experiments on a cart-pole system and a real quadruped robot demonstrate the distinguished features of the SeC-learning machine, compared with continual learning built on state-of-the-art safe DRL frameworks with approaches to addressing the Sim2Real gap.

## 1 Introduction

Deep reinforcement learning (DRL) has been integrated into many autonomous systems (see examples in Figure 1) and have demonstrated breakthroughs in sequential and complex decision-making in broad areas, ranging from autonomous driving [1, 2] to chemical processes [3, 4] to robot locomotion [5, 6]. Such learning-integrated systems promise to revolutionize many processes in different industries with tangible economic impact [7, 8]. However, the public-facing AI incident database [9] reveals that machine learning (ML) techniques, including DRL, can deliver remarkably high performance but no safety assurance [10]. Hence, the high-performance DRL with verifiable safety assurance is even more vital today, aligning well with the market’s need for safe ML technologies.

### 1.1 Related Work on Safe DRL

Significant efforts have been devoted to promoting safe DRL in recent years, including developing safety-embedded rewards and residual action policies and deriving verifiable safety, as detailed below.

The safety-embedded reward is crucial for a DRL agent to learn a high-performance action policy with verifiable safety. The control Lyapunov function (CLF) is the potential safety-embedded reward [11, 12, 13, 14]. Meanwhile, the seminal work [15] revealed that a CLF-like reward can enable DRL with verifiable stability. At the same time, enabling verifiable safety is achievable by extending CLF-like rewards with given safety conditions or regulations. However, systematic guidance for constructing such CLF-like rewards remains open.

37 The residual action policy is  
 38 another shift in the focus of  
 39 safe DRL, which integrates data-  
 40 driven DRL action policy and  
 41 physics-model-based action pol-  
 42 icy. The existing residual dia-  
 43 grams focus on stability guaran-  
 44 tee [16, 17, 18, 19], with the ex-  
 45 ception being [20] on safety guar-  
 46 antee. However, the physics mod-  
 47 els considered are nonlinear and  
 48 intractable, which thwarts deliv-  
 49 ering a verifiable safety guarantee  
 50 or assurance, if not impossible.

51 The verifiable safety (i.e., hav-  
 52 ing verifiable conditions of safety  
 53 guarantee) is enabled in the re-  
 54 cently developed Phy-DRL (physics-regulated DRL) framework [21, 22]. Meanwhile, Phy-DRL can  
 55 address the aforementioned open problems. Summarily, Phy-DRL simplifies a nonlinear system dy-  
 56 namics model as an analyzable and tractable linear one. This linear model can then be a model-based  
 57 guide for constructing the safety-embedded (CLF-like) reward and residual action policy.

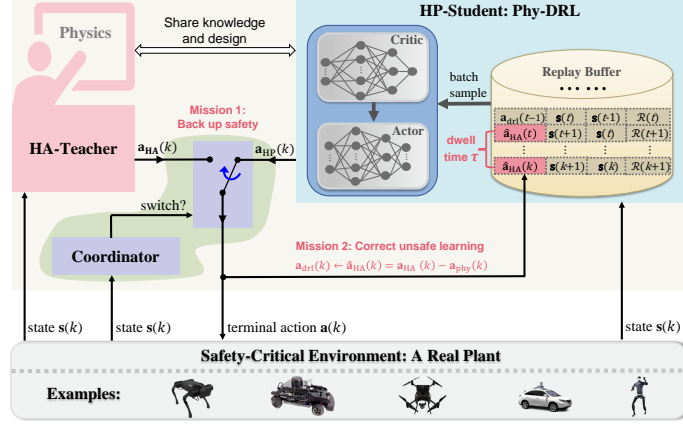


Figure 1: SeC-Learning Machine.

## 58 1.2 Challenges and Open Problems

59 Although safe DRL has developed significantly, DRL-enabled autonomous systems still face  
 60 formidable safety challenges, rooting in the Sim2Real gap and unknown unknowns on real plants.

61 **Challenge 1: Sim2Real Gap.** Due to the expense of data acquisition and potential safety concerns in  
 62 real-world settings, the prevalent DRL involves training a policy within a simulator using synthetic  
 63 data and deploying it onto the physical platforms. The discrepancy between the simulated environment  
 64 and the real scenario thus leads to the Sim2Real gap that degrades the performance of the pre-  
 65 trained DRL in a real plant. Numerous approaches have been developed to address Sim2Real gap  
 66 [23, 24, 25, 26, 27, 28, 29, 30, 31]. The common aim of these approaches is to enhance realism in  
 67 the simulator through, for example, domain randomization [32] and delay randomization (mimicking  
 68 asynchronous communication and sampling) [28]. These approaches can address the Sim2Real gap  
 69 to different degrees. However, the unrevealed gap still persistently impedes safety assurance if DRL  
 70 (also other ML) is not trained or learning in the real plant in real environments, using real-time data.

71 **Challenge 2: Unknown Unknowns.** The unknown unknowns generally refer to outcomes, events,  
 72 circumstances, or consequences that are not known in advance and cannot be predicted in time and  
 73 distributions [33]. The dynamics of many learning-enabled systems (e.g., autonomous vehicles [34]  
 74 and airplanes [35]) are governed by conjunctive known knowns (e.g., Newton’s laws of motion),  
 75 known unknowns (e.g., Gaussian noise without knowing mean and variance), and unknown unknowns  
 76 (due to, for example, unforeseen operating environments and DNNs’ huge parameter space, intractable  
 77 activation and hard-to-verify). The safety assurance also requires resilience to unknown unknowns,  
 78 which is very challenging. The reasons root in characteristics of unknown unknowns: almost zero  
 79 historical data and unpredictable time and distributions, leading to unavailable models for scientific  
 80 discoveries and understanding.

81 Intuitively, enabling the continual learning of the DRL agent in the real plant – using its real-time  
 82 data generated in real environments – is the way to address Challenges 1 and 2. However, two safety  
 83 problems related to the prospect of continual learning arise.

84 **Problem 1.1.** *How do we teach or assist the DRL agent to correct his unsafe continual learning?*

85 **Problem 1.2.** *Facing an unsafe DRL agent, how can we guarantee the real-time safety of a system?*

## 87 1.3 Contribution: Simplex-enabled Safe Continual Learning Machine

88 If successful, continual learning in a real plant can directly address the Sim2Real gap and learn to  
 89 tolerate unknown unknowns. However, the DRL’s real-time action policy during continual learning

cannot be fully verified and can have software faults. Continual learning shall run on a fault-tolerant architecture to address this safety concern. Simplex – using simplicity to control complexity [36, 37] – is a successful software architecture for complex safety-critical autonomous systems. The core of Simplex uses verified and simplified high-assurance controller to control the unverified high-performance and complex controller. Meanwhile, recently developed Phy-DRL theoretically and experimentally features fast training with verifiable safety [21, 22]. These motivate us to develop the **Simplex-enabled safe continual learning (SeC-learning) machine** to address Problem 1.1 and Problem 1.2, which is built on Simplex architecture and Phy-DRL. As shown in Figure 1, the SeC-learning machine constitutes HP (high performance)-Student, HA (high assurance)-Teacher, and coordinator. The HP-Student is a pre-trained Phy-DRL and continues to learn to tune the action policy to be safe in a real plant. The HA-Teacher action is a verified, mission-reduced, and physics-model-based design. As a complementary, HA-Teacher has two missions: backing up safety and teaching to correct unsafe learning of HP-Student. The coordinator triggers the switch and the interaction between the HP-Student and HA-Teacher to ensure lifetime safety (i.e., safety guarantee in any stage of continual learning, regardless of HP-Student’s success or convergence).

Note: Table 1 in Appendix A.1 summarizes notations used throughout the paper.

## 2 Preliminaries: Safety Definition

The dynamics of a real plant can be described by

$$\mathbf{s}(k+1) = \mathbf{A} \cdot \mathbf{s}(k) + \mathbf{B} \cdot \mathbf{a}(k) + \mathbf{f}(\mathbf{s}(k), \mathbf{a}(k)), \quad k \in \mathbb{N} \quad (1)$$

where  $\mathbf{f}(\mathbf{s}(k), \mathbf{a}(k)) \in \mathbb{R}^n$  is the unknown model mismatch,  $\mathbf{A} \in \mathbb{R}^{n \times n}$  and  $\mathbf{B} \in \mathbb{R}^{n \times m}$  denote known system matrix and control structure matrix, respectively,  $\mathbf{s}(k) \in \mathbb{R}^n$  is real-time system state of real plant,  $\mathbf{a}(k) \in \mathbb{R}^m$  is real-time action from SeC-learning machine.

The actions of the SeC-learning machine aims to constrain the states of a real plant to the safety set:

$$\text{Safety set : } \mathbb{X} \triangleq \{ \mathbf{s} \in \mathbb{R}^n \mid \underline{\mathbf{v}} \leq \mathbf{D} \cdot \mathbf{s} - \bar{\mathbf{v}} \leq \bar{\mathbf{v}}, \mathbf{D} \in \mathbb{R}^{h \times n}, \text{ with } \mathbf{v}, \bar{\mathbf{v}}, \underline{\mathbf{v}} \in \mathbb{R}^h \}. \quad (2)$$

where  $\mathbf{D}$ ,  $\mathbf{v}$ ,  $\bar{\mathbf{v}}$  and  $\underline{\mathbf{v}}$  are given in advance for formulating  $h \in \mathbb{N}$  safety conditions. In the SeC-learning machine, the safety set is not directly used to embed high-dimensional safety conditions (indicated by  $h \in \mathbb{N}$  in Equation (2)) into the DRL reward since the reward is a real one-dimensional value. To address the problem, the concept of safety envelope was introduced in [38, 21, 22], whose condition is one-dimensional and which will be designed to be a subset of the safety set  $\mathbb{X}$ .

$$\text{Safety envelope: } \Omega \triangleq \{ \mathbf{s} \in \mathbb{R}^n \mid \mathbf{s}^\top \cdot \mathbf{P} \cdot \mathbf{s} \leq 1, \mathbf{P} \succ 0 \}, \quad (3)$$

building on which safety definition is introduced below.

**Definition 2.1.** Consider the safety envelope  $\Omega$  (3) and safety set  $\mathbb{X}$  (2). The real plant (1) is said to be safe, if given any  $\mathbf{s}(1) \in \Omega \subseteq \mathbb{X}$ , the  $\mathbf{s}(k) \in \Omega \subseteq \mathbb{X}$  holds for any time  $k \in \mathbb{N}$ .

## 3 Design Overview: SeC-Learning Machine

The proposed SeC-learning machine aims to address Problem 1.1 and Problem 1.2 with capabilities of assuring lifetime safety, addressing the Sim2Real gap, and tolerating unknown unknowns. To do so, as shown in Figure 1, the learning machine is designed to have three critical interactive components:

- **HP-Student** is a pre-trained Phy-DRL (physics-regulated DRL [21, 22]) model and continues to learn in a safety-critical real plant to tune his action policy to be safe.
- **HA-Teacher** is a verifiable and analyzable physics-model-based action policy with two missions: backing up the safety of a real plant and correcting unsafe learning of HP-Student.
- **Coordinator** triggers the switch and interaction between HP-Student and HA-Teacher by monitoring the real-time system states. Specifically, when the real-time states of the real plant under the control of HP-Student approach the safety boundary, the coordinator triggers the switch to HA-Teacher and the correction of unsafe actions in learning. In other words, the HA-Teacher takes over the HP-Student to control the real plant to safe (i.e., backing up safety). Meanwhile, the HA-Teacher uses his safe actions to correct the HP-Student’s unsafe actions in the replay buffer for learning. Once the real-time states return to a safe region, the coordinator triggers the switch back to HP-Student and terminates the learning correction.

Next, we detail the designs of the three interactive components in Sections 4 to 6, respectively.

## 4 SeC-Learning Machine: HP-Student Component

The HP-Student builds on Phy-DRL (physics-regulated deep reinforcement learning) proposed in [21, 22]. The critical reason is that Phy-DRL’s training mission is pre-defined: searching for an action policy that renders the assigned safety envelope invariant. In this way, HP-Student can share his mission with HP-Student and Coordinator, so they can have a common goal in the learning machine: rendering the safety envelope invariant in a safety-critical real plant in the face of Sim2Real gap and unknown unknowns. We next detail the designs of HP-Student.

### 4.1 HP-Student: Residual Action Policy and Safety-embedded Reward

Following Phy-DRL in [21, 22], the HP-Student adopts the concurrent residual action policy and safety-embedded reward, as they can offer fast and stable training and successfully encode the safety envelope  $\Omega$ . The residual action formula is

$$\mathbf{a}_{\text{HP}}(k) = \underbrace{\mathbf{a}_{\text{drl}}(k)}_{\text{data-driven}} + \underbrace{\mathbf{a}_{\text{phy}}(k)}_{\text{model-based}} (:= \mathbf{F} \cdot \mathbf{s}(k)), \quad (4)$$

where  $\mathbf{a}_{\text{drl}}(k)$  denotes a data-driven action from DRL, while  $\mathbf{a}_{\text{phy}}(k)$  is a physics-model-based action ( $\mathbf{F}$  is our design). Meanwhile, the safety-embedded reward:

$$\mathcal{R}(\mathbf{s}(k), \mathbf{a}_{\text{drl}}(k)) = \underbrace{\mathbf{s}^\top(k) \cdot \mathbf{H} \cdot \mathbf{s}(k) - \mathbf{s}^\top(k+1) \cdot \mathbf{P} \cdot \mathbf{s}(k+1)}_{\triangleq r(\mathbf{s}(k), \mathbf{s}(k+1))} + w(\mathbf{s}(k), \mathbf{a}_{\text{HP}}(k)), \quad (5)$$

where the sub-reward  $w(\mathbf{s}(k), \mathbf{a}(k))$  aims at high-performance operations (e.g., minimizing energy consumption of resource-limited robots [39, 40]). In contrast, the sub-reward  $r(\mathbf{s}(k), \mathbf{s}(k+1))$  is safety-critical. Equation (5) also defines:

$$\mathbf{H} \triangleq \mathbf{A}^\top \cdot \mathbf{P} \cdot \mathbf{A}, \quad \text{with } \mathbf{A} \triangleq \mathbf{A} + \mathbf{B} \cdot \mathbf{F} \text{ and } 0 \prec \mathbf{H} \prec \alpha \cdot \mathbf{P}, \quad \alpha \in (0, 1). \quad (6)$$

The matrices  $\mathbf{P}$  and  $\mathbf{F}$  are design variables, using the available physics-model knowledge ( $\mathbf{A}$ ,  $\mathbf{B}$ ). Their automatic computations will be discussed in Section 4.2.

### 4.2 HP-Student: Controllable Contribution Ratio

In residual diagram (4), the contribution ratio between data-driven and model-based policies controls HP-Student’s safety and system performance. To understand this, we define the contribution ratio as  $\gamma \triangleq \frac{\text{space}\{\mathbf{a}_{\text{drl}}(k), \forall k \in \mathbb{N}\}}{\text{space}\{\mathbf{a}_{\text{drl}}(k), \forall k \in \mathbb{N}\} + \text{space}\{\mathbf{a}_{\text{phy}}(k), \forall k \in \mathbb{N}\}}$ . As depicted in Figure 2, if  $\gamma$  approaches 0, i.e., the physics-model-based

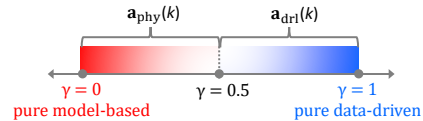


Figure 2: Contribution ratio  $\gamma$ .

action policy dominates the integration, featuring analyzable and verifiable behavior but limited performance. If  $\gamma$  approaches 1, i.e., the data-driven policy dominates the integration, featuring high performance but hard-to-analyze and hard-to-verify. Therefore, a controllable contribution ratio is desired. The controllable space of data-driven actions is innate, as Phy-DRL is built on DDPG [41], which directly maps states to actions within the interval  $[-1, 1]$  using the Tanh activation function. The action space can be rescaled with a controllable magnitude factor  $m$  to expand the space to  $[-m, m]$ . So, the remaining job is to enable the controllable space of physics-model-based actions:

$$\text{Action Space: } \mathbb{A}_{\text{phy}} \triangleq \{ \mathbf{a}_{\text{phy}} \in \mathbb{R}^m \mid \underline{\mathbf{z}} \leq \mathbf{C} \cdot \mathbf{a}_{\text{phy}} - \mathbf{z} \leq \bar{\mathbf{z}}, \text{ with } \mathbf{C} \in \mathbb{R}^{g \times m}, \mathbf{z}, \bar{\mathbf{z}}, \underline{\mathbf{z}} \in \mathbb{R}^m \}. \quad (7)$$

where  $\mathbf{C}$ ,  $\mathbf{z}$ ,  $\bar{\mathbf{z}}$  and  $\underline{\mathbf{z}}$  are users’ options for controlling the space of model-based actions. Equation (4) shows the model-based action completely depends on  $\mathbf{F}$ . So, we shall redesign  $\mathbf{F}$  to control model-based action to space (7). Due to the page limit, the proposed redesign for delivering  $\mathbf{F}$ , reward (5) and controllable action space (7) is presented in Appendix C.2.

### 4.3 HP-Student: Continual Learning

HP-Student is a Phy-DRL model pre-trained in a simulator or another domain, which takes the *actor-critic* architecture-based DRLs such as [41] [42] for training. The pre-trained Phy-DRL model has an

176 action policy and an action-value function. When deployed to a new safety-critical environment, the  
 177 SeC-learning machine enables the pre-trained policy to continually and safely search for a safe policy  
 178 that maximizes the expected return.

179 Sampling efficiency is one of the important considerations for continual learning in the real world.  
 180 Experience replay (ER) [43] allows off-policy algorithms to reuse the experience collected in the  
 181 past, greatly improving the sampling efficiency and avoiding forgetting the learned knowledge [44].  
 182 ER is also beneficial for breaking the correlation between adjacent transitions to avoid sampling bias  
 183 for a stable learning process. Those features are very important in continual learning, where online  
 184 data is limited due to the expensive interaction on the physical system. During the online inference,  
 185 we continuously store the real transitions realized by safe high-performance action of HP-Student or  
 186 corrected unsafe data-driven action by HA-Teacher to the replay buffer. Specifically, as illustrated in  
 187 Figure 1, if the HP-Student's action  $\mathbf{a}_{\text{HP}}(k)$  leads to unsafe behavior of a real plant, HA-Teacher takes  
 188 over his role of controlling real plant to be safe, and corrects his unsafe data-driven action  $\mathbf{a}_{\text{drl}}(k)$  to  
 189  $\hat{\mathbf{a}}_{\text{HA}}(k)$  according to

$$\mathbf{a}_{\text{drl}}(k) \leftarrow \hat{\mathbf{a}}_{\text{HA}}(k) \triangleq \mathbf{a}_{\text{HA}}(k) - \mathbf{a}_{\text{phy}}(k), \quad (8)$$

190 where  $\mathbf{a}_{\text{phy}}(k)$  is HP-student's model-based action in residual action policy (4), and  $\mathbf{a}_{\text{HA}}(k)$  is the  
 191 action from HA-Teacher, whose design is presented in Section 6. Meanwhile, the online learning  
 192 process will uniformly sample a minibatch of transitions for learning or training [45].

193 **Remark 4.1.** Equation (8) indicates that for HP-Student's residual action policy (4), the correction  
 194 is performed only on data-driven action  $\mathbf{a}_{\text{drl}}(k)$ , i.e., not including model-based action  $\mathbf{a}_{\text{phy}}(k)$ . The  
 195 reason is that although the model-based design has limited performance and a small safe operation  
 196 region due to model mismatch, it is analyzable and verifiable, and its policy is invariant because of  
 197 his invariant physics-model knowledge ( $\mathbf{A}$ ,  $\mathbf{B}$ ).

## 198 5 SeC-Learning Machine: Coordinator Component

199 The Coordinator triggers the switch between HP-Student and HA-Teacher to control the real plant by  
 200 monitoring the system's state in real-time. The switching logic of terminal action applied to a real  
 201 plant is described below.

$$\mathbf{a}(k) = \begin{cases} \mathbf{a}_{\text{HA}}(k), & \text{if } \mathbf{s}^\top(t) \cdot \mathbf{P} \cdot \mathbf{s}(t) \geq \varepsilon < 1 \text{ and } t \leq k \leq t + \tau, \tau \in \mathbb{N} \\ \mathbf{a}_{\text{HP}}(k), & \text{otherwise} \end{cases} \quad (9)$$

202 synchronizing with which is the correcting logic of HP-Student's unsafe actions in his replay buffer:

$$\mathbf{a}_{\text{drl}}(k) = \begin{cases} \hat{\mathbf{a}}_{\text{HA}}(k), & \text{if } \mathbf{s}^\top(t) \cdot \mathbf{P} \cdot \mathbf{s}(t) \geq \varepsilon < 1 \text{ and } t \leq k \leq t + \tau, \tau \in \mathbb{N} \\ \mathbf{a}_{\text{drl}}(k), & \text{otherwise} \end{cases} \quad (10)$$

203 where  $\hat{\mathbf{a}}_{\text{HA}}(k)$  is the corrected unsafe action by HA-Teacher, defined in Equation (8). Noting that  
 204 real plant initially operates from a safety  
 205 envelope, we can observe from Equation (9) and Equation (10) that the trig-  
 206 gering condition of the switch from HP-  
 207 Student to HA-Teacher and the unsafe  
 208 action correction is  $\mathbf{s}^\top(t) \cdot \mathbf{P} \cdot \mathbf{s}(t) \geq \varepsilon$ .  
 209 In addition, the requirement ' $t \leq k \leq$   
 210  $t + \tau$ ' indicates that once HA-Teacher  
 211 takes over the role of HP-Student, he  
 212 has a dwell time  $\tau \in \mathbb{N}$ ; after the dwell  
 213 time, he returns the control role to HP-  
 214 Student. The dwell time has two considerations:

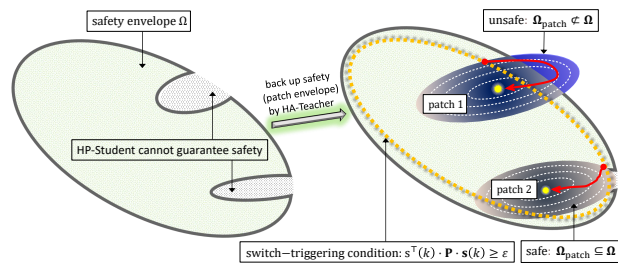


Figure 3: System phase behavior.

- 216 • Constraining the states of a real plant to a very safe space (i.e., approaching the center of a  
 217 safety envelope patch, illustrated in Figure 3) to preserve sufficient fault-tolerant space for  
 218 HP-Student's continual learning.
- 219 • Collecting sufficient data of safe actions and states to correct the unsafe continual learning  
 220 of HP-Student (see corrected  $\tau \in \mathbb{N}$  unsafe actions in replay buffer in Figure 1).

221 The dwell time  $\tau$  is a design of HA-Teacher, which is carried out in Equation (21) in Remark 6.3.

**Remark 5.1 (Parallel Running).** Finally, we note that the HA-Teacher and HP-Student in the SeC-learning machine run in parallel. This configuration guarantees that when the HA Teacher is activated by the Coordinator to back up safety and correct unsafe learning, his actions can be available immediately. If operating without parallel running, the system can lose control due to the time delay in sampling, communication, and computation.

## 6 SeC-Learning Machine: HA-Teacher Component

HA-Teacher has tasks in the SeC-learning machine:

- **Back up Safety via Patching Safety Envelope.** As soon as the HP-Student leads to an unsafe real-time system behavior, the HA-Teacher intervenes to safely control the system through patching the safety envelope, depicting in Figure 3.
- **Correct Unsafe Learning.** The HA-Teacher uses safe actions to correct the real-time and potentially (in dwell time  $\tau$  horizon) unsafe actions of the HP-Student for learning.

HA-Teacher is a physics-model-based design whose function is reduced to be safety-critical only. Compared with the HP-Student, the HA-Teacher has relatively rich dynamics knowledge about real plants. Hereto, the dynamics model leveraged by HA-Teacher updates from (1) as

$$\mathbf{s}(k+1) = \mathbf{A}(\mathbf{s}(k)) \cdot \mathbf{s}(k) + \mathbf{B}(\mathbf{s}(k)) \cdot \mathbf{a}_{\text{HA}}(k) + \mathbf{g}(\mathbf{s}(k)), \quad k \in \mathbb{N} \quad (11)$$

where  $\mathbf{g}(\mathbf{s}(k)) \in \mathbb{R}^n$  is the unknown model mismatch for HA-Teacher. The physics-model knowledge available to HA-Teacher is thus  $(\mathbf{A}(\mathbf{s}(k)), \mathbf{B}(\mathbf{s}(k)))$ . Because of the **Parallel Running** configuration, HA-Teacher is always active to compute a safe action policy with control goal as

$$\text{Patch center : } \bar{\mathbf{s}}^* = \chi \cdot \mathbf{s}(k) \quad \text{with } \chi \in (-1, 1). \quad (12)$$

In other words, with real-time sensor data and physics-model knowledge, the HA-Teacher is always in ‘active’ status to compute a model-based action policy to control the real plant to reach the goal  $\bar{\mathbf{s}}^*$ . To achieve this, HA-Teacher first obtains tracking-error dynamics from Equation (11) as

$$\mathbf{e}(k+1) = \mathbf{A}(\mathbf{s}(k)) \cdot \mathbf{e}(k) + \mathbf{B}(\mathbf{s}(k)) \cdot \mathbf{a}_{\text{HA}}(k) + \mathbf{h}(\mathbf{e}(k)), \quad \text{with } \mathbf{e}(k) \triangleq \mathbf{s}(k) - \bar{\mathbf{s}}^* \quad (13)$$

where  $\mathbf{h}(\mathbf{e}(k)) \in \mathbb{R}^n$  denotes unknown model mismatch, and HA-Teacher’s action policy is

$$\mathbf{a}_{\text{HA}}(k) = \hat{\mathbf{F}} \cdot \mathbf{e}(k), \quad (14)$$

whose aim is to track the goal  $\bar{\mathbf{s}}^*$  while constraining system states to the envelope patch:

$$\text{Envelope patch: } \Omega_{\text{patch}} \triangleq \left\{ \mathbf{s} \mid (\mathbf{s} - \bar{\mathbf{s}}^*)^\top \cdot \hat{\mathbf{P}} \cdot (\mathbf{s} - \bar{\mathbf{s}}^*) \leq (1 - \chi)^2 \cdot \mathbf{s}^\top(k) \cdot \hat{\mathbf{P}} \cdot \mathbf{s}(k), \quad \hat{\mathbf{P}} \succ 0 \right\}. \quad (15)$$

The matrices  $\hat{\mathbf{F}}$  and  $\hat{\mathbf{P}}$  in Equation (14) and Equation (15) are HA-Teacher’s design variables for backing up safety and correcting unsafe learning. To have them, we present a practical and common assumption on unknown model mismatch for computing them.

**Assumption 6.1.** The model mismatch in  $\mathbf{h}(\cdot)$  in Equation (13) is locally Lipschitz in set  $\Omega_{\text{patch}}$ , i.e.,

$$(\mathbf{h}(\mathbf{e}_1) - \mathbf{h}(\mathbf{e}_2))^\top \cdot \mathbf{P} \cdot (\mathbf{h}(\mathbf{e}_1) - \mathbf{h}(\mathbf{e}_2)) \leq \kappa \cdot (\mathbf{e}_1 - \mathbf{e}_2)^\top \cdot \mathbf{P} \cdot (\mathbf{e}_1 - \mathbf{e}_2), \quad \forall \mathbf{e}_1, \mathbf{e}_2 \in \Omega_{\text{patch}},$$

where  $\mathbf{P} \succ 0$  is shared by HP-Student, which defines his safety envelope (3) and safety-embedded reward (5).

The designs of  $\hat{\mathbf{F}}$  and  $\hat{\mathbf{P}}$  for delivering HA-Teacher’s capabilities of backing up safety and correcting unsafe learning are formally presented in the following theorem, whose proof appears in Appendix D.

**Theorem 6.2.** Consider the HA-Teacher’s action policy (14) and the envelope patch  $\Omega_{\text{patch}}$  (15), whose matrices  $\hat{\mathbf{F}}$  and  $\hat{\mathbf{P}}$  are computed according to

$$\hat{\mathbf{F}} = \hat{\mathbf{R}} \cdot \hat{\mathbf{Q}}^{-1}, \quad \hat{\mathbf{P}} = \hat{\mathbf{Q}}^{-1}, \quad (16)$$

with the matrices  $\hat{\mathbf{R}}$  and  $\hat{\mathbf{Q}}$  satisfying

$$\hat{\mathbf{Q}} \cdot \mathbf{P} \prec \mathbf{I}_n \prec \eta \cdot \hat{\mathbf{Q}} \cdot \mathbf{P}, \quad \text{with a given } \eta > 1 \quad (17)$$

$$\begin{bmatrix} (\beta - \kappa \cdot \eta \cdot (1 + \frac{1}{\omega})) \cdot \hat{\mathbf{Q}} & \hat{\mathbf{Q}} \cdot \mathbf{A}^\top(\mathbf{s}(k)) + \hat{\mathbf{R}}^\top \cdot \mathbf{B}^\top(\mathbf{s}(k)) \\ \mathbf{A}(\mathbf{s}(k)) \cdot \hat{\mathbf{Q}} + \mathbf{B}(\mathbf{s}(k)) \cdot \hat{\mathbf{R}} & \frac{\hat{\mathbf{Q}}}{1+\omega} \end{bmatrix} \succ 0, \quad (18)$$

where  $\beta \in (0, 1)$  and  $\omega > 0$  are given parameters. Under Assumption 6.1, the system (13) controlled by HA-Teacher has the following properties:

- 258 1. The  $\mathbf{e}^\top(k+1) \cdot \hat{\mathbf{P}} \cdot \mathbf{e}(k+1) \leq \beta \cdot \mathbf{e}^\top(k) \cdot \hat{\mathbf{P}} \cdot \mathbf{e}(k)$  holds for any  $k \in \mathbb{N}$ .  
 259 2. The  $\Omega_{\text{patch}} \subseteq \Omega$  holds if the parameters  $\eta$  in Equation (17) and  $\chi$  in Equation (12) satisfy  

$$(1 - \chi)^2 \cdot \eta \cdot \varepsilon + \chi^2 \cdot \varepsilon \leq 0.5. \quad (19)$$

260  
 261 **Remark 6.3 (Suggestion from Item 1: Dwell time  $\tau$  of HA-Teacher).** We obtain from Item 1 that

$$\mathbf{e}^\top(k) \cdot \hat{\mathbf{P}} \cdot \mathbf{e}(k) \leq \beta^{k-t} \cdot (\mathbf{e}^*)^\top \cdot \hat{\mathbf{P}} \cdot (\mathbf{e}^*), \quad (20)$$

262 wherein the  $t$  and  $\mathbf{e}^*$  denote the activation time of HA-Teacher and the initial distance with goal  
 263  $\bar{\mathbf{s}}^*$  (12), respectively. The real-time tracking error  $\mathbf{e}(k)$  can be understood as the distance to the  
 264 goal  $\bar{\mathbf{s}}^*$  (i.e., the center of envelope patch). Meanwhile, we can use  $\mathbf{e}^\top(k) \cdot \hat{\mathbf{P}} \cdot \mathbf{e}(k)$  as distance  
 265 function or performance metric. Hereto, we consider a safety criteria as  $\mathbf{e}^\top(k) \cdot \hat{\mathbf{P}} \cdot \mathbf{e}(k) \leq \delta$ .  
 266 Illustrated in Figure 3, a very small  $\delta$  means “being very close to patch center” and that HA-Teacher  
 267 can preserve sufficient fault-tolerance space for HA-Teacher’s continual learning. Meanwhile, when  
 268 the preset safety criteria hold, HP-Student takes back the control role from HA-Teacher. According to  
 269 Equation (20), the condition of HA-Teacher’s dwell time for satisfying the safety criteria is

$$\tau \geq \left\lceil \frac{\ln \delta - \ln (\mathbf{e}^*)^\top \cdot \hat{\mathbf{P}} \cdot (\mathbf{e}^*)}{\ln \beta} \right\rceil. \quad (21)$$

270 In other words, if  $k - t \geq \tau$  and  $\tau$  satisfies Equation (21), we have  $\mathbf{e}^\top(k) \cdot \hat{\mathbf{P}} \cdot \mathbf{e}(k) \leq \delta$ .

271 **Remark 6.4 (Suggestion from Item 2: Backing up safety by envelope patches).** Condition (18) is  
 272 for backing up safety when the HP-Student’s actions cannot guarantee real plants’ real-time safety.  
 273 As depicted in Figure 3, if only the property in Item 1 of Theorem C.1 holds, the HA-Teacher cannot  
 274 back up safety due to the unsafe region, highlighted in blue color. Only after the Item 2 of Theorem C.1  
 275 holds can HA-Teacher achieve the concurrent missions of backing up safety and correcting learning,  
 276 as the unsafe regions (i.e., regions outside the safety envelope) disappear.

277 **Remark 6.5 (Fast Computation).** The  $\hat{\mathbf{F}}$  and  $\hat{\mathbf{P}}$  are automatically computed from inequalities (17)  
 278 and (18) by LMI toolbox [46, 47]. Its computation time is usually significantly small (e.g., 0.01 sec –  
 279 0.04 sec), and its influence can be ignored in the configuration of parallel running (see Remark 5.1).

280 **Remark 6.6 (Extreme Case: Fast Model Learning).** In the extreme case that the HA-Teacher has  
 281 zero knowledge about  $(\mathbf{A}(\mathbf{s}(k)), \mathbf{B}(\mathbf{s}(k)))$ . Learning them online is needed. Fast model learning  
 282 (using only a few most recently generated sensor data) proposed in [38] is an approach to have them  
 283 online timely. The approach is presented in Appendix E.

## 284 7 Experiment

285 We perform the experiments on a cart-pole system (simulator) and a real quadruped robot.

### 286 7.1 Cart-Pole System

287 This experiment aims to demonstrate the effectiveness of the SeC-Learning Machine from perspectives  
 288 of concurrent safety and training performances in the face of the Sim2Real gap. The pre-training  
 289 of HP-Student (i.e., Phy-DRL) is performed on the simulator provided in Open-AI Gym [48]. To  
 290 address the Sim2Real gap, the pre-training adopts domain randomization [32, 24] through introducing  
 291 random force disturbances and randomizing friction force. We also use the simulator to mimic a  
 292 real plant whose Sim2Real gap is intentionally created by inducing a friction force that is out of the  
 293 distribution of the random friction force used in pre-training.

294 The system’s mechanical analog is characterized by the pendulum’s angle  $\theta$ , the cart’s position  $x$ ,  
 295 and their velocities  $\omega = \dot{\theta}$  and  $v = \dot{x}$ . The mission of HP-Student is to stabilize the pendulum at  
 296 equilibrium  $\mathbf{s}^* = [0, 0, 0, 0]^\top$  while constraining the system state to safety set:

$$\mathbb{X} = \{ \mathbf{s} \in \mathbb{R}^4 \mid -0.9 \leq x \leq 0.9, \quad -0.8 < \theta < 0.8 \}. \quad (22)$$

297 Given the safety set, we set the space of physics-model-based action policy as

$$\mathbb{A}_{\text{phy}} \triangleq \{ \mathbf{a}_{\text{phy}} \in \mathbb{R} \mid -25 \leq \mathbf{a}_{\text{phy}} \leq 25 \}. \quad (23)$$

298 With them, the designs of HP-Student and HA-Teacher are presented in Appendix F.3 and Ap-  
 299 pendix F.4, respectively.



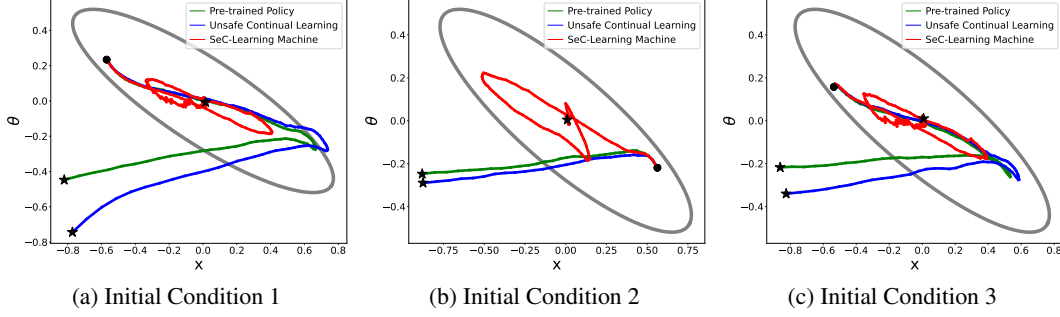


Figure 5: **Two Episodes**. Phase plots, given the same initial condition. The black dot and star denote the initial condition and final location, respectively.

For continual learning in mimicked real plants, the maximum length of one episode is 1500 steps. For the comparisons, we consider three models: ‘*Pre-trained Policy*’ (i.e., Phy-DRL pre-trained in a simulator, using randomization approaches for addressing Sim2Real gap), ‘*Unsafe Continual Learning*’ (i.e., pre-trained Phy-DRL continues to learn in the real plant but no Simplex support), and our proposed ‘*SeC-Learning Machine*’. A very distinguished feature of our SeC-Learning Machine is lifetime safety, i.e., a safety guarantee in any stage of continual learning, regardless of the success of HP-Student. To demonstrate this and have fair comparisons, HP-Student in the ‘*SeC-Learning Machine*’ and the ‘*Unsafe Continual Learning*’ model are picked after training for **only two episodes**. Given the three different initial conditions, phases plots of these three models are shown in Figure 5. To further convincingly demonstrate the feature, additional phase plots are shown in Figure 7, Figure 8, and Figure 9, where the models are picked after training for only **three episodes**, **four episodes**, **five episodes**, respectively. Meanwhile, the reward’s training curves (five random seeds) are shown in Figure 4. Observing Figures 4, 5 and 7 to 9, we conclude:

- In the face of a large Sim2Real gap with a pre-training environment, the SeC-Learning Machine can always guarantee safety (system states never leave the safety envelope; see red curves in Figures 5 and 7 to 9) in any stage of continual learning. In contrast, the pre-trained model and continual learning without Simplex cannot guarantee safety (system states left the safety envelope; see blue and green curves in Figures 5 and 7 to 9).
- Unsafe action correction and safety backup from HA-Teacher lead to remarkably stable and fast training, compared with continual learning without Simplex logic (see Figure 4).

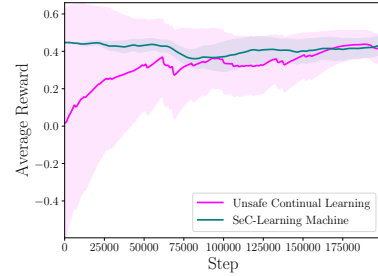


Figure 4: Episode reward.

## 7.2 Real Quadruped Robot

The mission of the action policy is to control the robot’s COM height, COM x-velocity, and other states to track the corresponding commands  $r_{v_x}$ ,  $r_h$ , and zeros, under safety constraints:  $|\text{yaw}| \leq 0.2$  rad,  $|\text{CoM x-velocity} - r_{v_x}| \leq |r_{v_x}|$ ,  $|\text{CoM z-height} - r_h| \leq 0.12$  m, and  $|\text{CoM yaw velocity}| \leq 0.3$  rad/s. For the Coordinator’s switching logic (9) and correcting logic (10), we let  $\varepsilon = 0.65$  and  $\tau = 10$ . The designs of HP-Student and HA-Teacher are presented in Appendix G.3 and Appendix G.4, respectively. For HP-Student’s pre-training of addressing the Sim2Real gap, we consider the approaches of delay randomization proposed in [28] and force randomization. During pre-training in the simulator, the ground friction is set as 0.7, and  $r_{v_x} = 0.6$  m/s and  $r_h = 0.24$  m. In the real quadruped robot, one episode is defined as “running the robot for 15 sec.” To better demonstrate the performance of the SeC-Learning Machine, the velocity command for the real robot is  $r_{v_x} = 0.35$  m/s, which very different from the one for HP-Student’s training in the simulator.

We compare three models in the real quadruped robot: ‘*Phy-DRL*’ (a pre-trained Phy-DRL model in the simulator, directly deployed on the real robot), ‘*Continual Learning*’ (a pre-trained Phy-DRL model in simulator that continues learning in the real robot for 20 episodes but without Simplex logic), and our proposed ‘*SeC-Learning Machine*’ in the 1st episode in real robot. We consider the 1st episode for the ‘*SeC-Learning Machine*’ model, owing to its claimed feature of lifetime safety, i.e., safety guarantee in any stage of continual learning in a real plant regardless of HP-Student’s



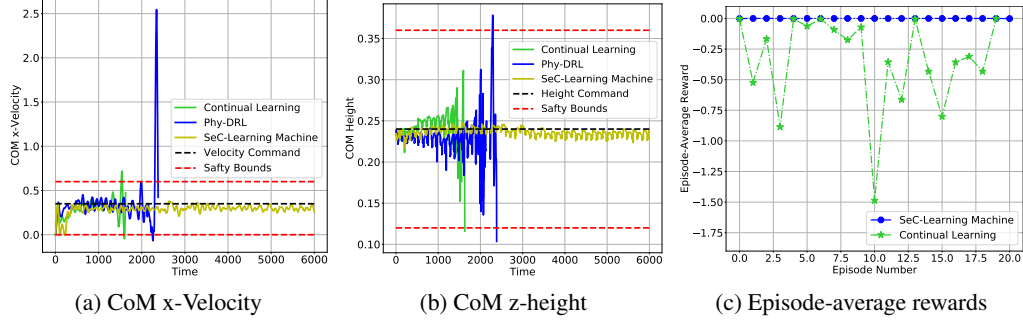


Figure 6: Comparisons of trajectories and episode-average reward.

convergence or success. Therefore, showing system trajectories in the 1st episode will be most convincing, as HP-Student cannot converge so fast for a safe action policy within only one episode. We also note that Phy-DRL or HP-Student is pre-trained well in the simulator, which can be viewed from video available at [simulator-video link \[anonymous hosting and browsing\]](#).

The comparisons are first viewed from the trajectories of the robot’s CoM height and x-velocity regarding tracking performance and safety guarantee, which are shown in Figure 6 (a) and (b). Meanwhile, the comparison video of the three models in real robots is available at [real-robot-video-1 link \[anonymous hosting and browsing\]](#). In addition, the real robot’s trajectories under the control of the SeC-Learning Machine in the 5th episode, 10th episode, 15th episode, and 20th episode are shown in Figures 10 to 13 in Appendix G.5.1, respectively. These figures straightforwardly depict that the SeC-Learning Machine guarantees the safety of real robots across all selected episodes or stages of continual learning. Observing Figure 6 (a) and (b), Figures 10 to 13, and the comparison video, we discover that Phy-DRL (i.e., HP-Student), a well pre-trained model in simulator, cannot guarantee the safety of the real robot due to the existing Sim2Real gap or unknown unknowns in the physical environment that the delay and force randomization failed to capture. Thus, continuous real-time learning is needed for the real robot. However, without Simplex logic, the safety of real robot during continual learning is not guaranteed. The SeC-Learning Machine successfully addresses these challenges by ensuring lifetime safety for continual real-time learning.

Finally, we emphasize that another critical mission of HA-Teacher is correcting HP-Student’s unsafe behavior. In other words, HP-Student learns from HA-Teacher to be safe when his actions are unsafe. To demonstrate this, we compare the episode-average reward curves of HP-Student (with HA-Teacher support) against the one (without Simplex logic or HA-Teacher support) in continual learning, as depicted in Figure 6 (c). In addition, the reward curves in the iteration step for 20 episodes are shown in Figure 14 in Appendix G.5.2. Meanwhile, We also deactivate HA-Teacher during the 20th episode of HP-Student’s continual learning to verify if HP-Student has quickly assimilated safe behaviors from HA-Teacher. The demonstration video for comparison with the initial HP-Student is available at [real-robot-video-2 link \[anonymous hosting and browsing\]](#). The demonstration video, Figure 6 (c) and Figure 14 prove that compared with Continual Learning, HA-Teacher enables stable, fast, and safe learning for HP-Student. Notably, the video shows that after only 20 episodes (i.e., 300 sec), the HP-Student has successfully learned from HA-Teacher to be safe.

## 8 Conclusion and Discussion

This paper develops the SeC-learning machine for safety-critical autonomous systems. The SeC-learning machine constitutes HP-Student (a pre-trained Phy-DRL, continuing to learn in a real plan), HA-Teacher (verified physics-model-based design), and Coordinator. In the learning machine, the HA-Teacher backs up safety and corrects unsafe learning of HP-Student. The SeC-learning machine aims to assure lifetime safety, address the Sim2Real gap, and learn to tolerate unknowns unknowns in real plants. Experiments also demonstrate that the SeC-learning machine features remarkably fast, stable, and safe training compared with continual learning without Simplex logic.

Intuitively, the SeC-learning machine is also an automatic hierarchy learning machine. Specifically, the HP-student first learns from the HA-teacher to be safe. If safe enough, i.e., the HP-student can be independent of the HA-teacher, the HP-student will learn by himself to achieve the goal of high performance with verifiable safety. This investigation continues our future research direction.

## References

- [1] Alex Kendall, Jeffrey Hawke, David Janz, Przemyslaw Mazur, Daniele Reda, John-Mark Allen, Vinh-Dieu Lam, Alex Bewley, and Amar Shah. Learning to drive in a day. In *2019 International Conference on Robotics and Automation*, pages 8248–8254. IEEE, 2019.
- [2] B Ravi Kiran, Ibrahim Sobh, Victor Talpaert, Patrick Mannion, Ahmad A Al Sallab, Senthil Yogamani, and Patrick Pérez. Deep reinforcement learning for autonomous driving: A survey. *IEEE Transactions on Intelligent Transportation Systems*, 23(6):4909–4926, 2021.
- [3] Thomas Savage, Dongda Zhang, Max Mowbray, and Ehecatl Antonio Del Río Chanona. Model-free safe reinforcement learning for chemical processes using gaussian processes. *IFAC-PapersOnLine*, 54(3):504–509, 2021.
- [4] Zhenglei He, Kim-Phuc Tran, Sebastien Thomassey, Xianyi Zeng, Jie Xu, and Changhai Yi. A deep reinforcement learning based multi-criteria decision support system for optimizing textile chemical process. *Computers in Industry*, 125:103373, 2021.
- [5] Julian Ibarz, Jie Tan, Chelsea Finn, Mrinal Kalakrishnan, Peter Pastor, and Sergey Levine. How to train your robot with deep reinforcement learning: lessons we have learned. *The International Journal of Robotics Research*, 40(4-5):698–721, 2021.
- [6] Sergey Levine, Chelsea Finn, Trevor Darrell, and Pieter Abbeel. End-to-end training of deep visuomotor policies. *The Journal of Machine Learning Research*, 17(1):1334–1373, 2016.
- [7] Tian Tolentino. Autonomous aircraft market worth usd 23.7bn by 2030. <https://www.traveldailymedia.com/autonomous-aircraft-market-research/>, 2019.
- [8] Bernard Marr. How Tesla is using artificial intelligence to create the autonomous cars of the future. *Bernard Marr & Co.* <https://bernardmarr.com/how-tesla-is-using-artificial-intelligence-to-create-the-autonomous-cars-of-the-future/>, 2021.
- [9] AI incident database. <https://incidentdatabase.ai/entities/>.
- [10] Arnold Zachary and Toner Helen. AI Accidents: An emerging threat. *Center for Security and Emerging Technology*, 2021.
- [11] Theodore J Perkins and Andrew G Barto. Lyapunov design for safe reinforcement learning. *Journal of Machine Learning Research*, 3(Dec):803–832, 2002.
- [12] Felix Berkenkamp, Matteo Turchetta, Angela Schoellig, and Andreas Krause. Safe model-based reinforcement learning with stability guarantees. *Advances in Neural Information Processing Systems*, 30, 2017.
- [13] Ya-Chien Chang and Sicun Gao. Stabilizing neural control using self-learned almost Lyapunov critics. In *2021 IEEE International Conference on Robotics and Automation*, pages 1803–1809. IEEE, 2021.
- [14] Liqun Zhao, Konstantinos Gatsis, and Antonis Papachristodoulou. Stable and safe reinforcement learning via a Barrier-Lyapunov actor-critic approach. In *62nd IEEE Conference on Decision and Control*, pages 1320–1325. IEEE, 2023.
- [15] Tyler Westenbroek, Fernando Castaneda, Ayush Agrawal, Shankar Sastry, and Koushil Sreenath. Lyapunov design for robust and efficient robotic reinforcement learning. *arXiv:2208.06721*, 2022.
- [16] Krishan Rana, Vibhavari Dasagi, Jesse Haviland, Ben Talbot, Michael Milford, and Niko Sünderhauf. Bayesian controller fusion: Leveraging control priors in deep reinforcement learning for robotics. *arXiv preprint* <https://arxiv.org/pdf/2107.09822.pdf>.
- [17] Tongxin Li, Ruixiao Yang, Guannan Qu, Yiheng Lin, Steven Low, and Adam Wierman. Equipping black-box policies with model-based advice for stable nonlinear control. *arXiv preprint* <https://arxiv.org/pdf/2206.01341.pdf>.

- 430 [18] Richard Cheng, Abhinav Verma, Gabor Orosz, Swarat Chaudhuri, Yisong Yue, and Joel Burdick.  
431 Control regularization for reduced variance reinforcement learning. In *International Conference*  
432 *on Machine Learning*, pages 1141–1150, 2019.
- 433 [19] Tobias Johannink, Shikhar Bahl, Ashvin Nair, Jianlan Luo, Avinash Kumar, Matthias Loskyll,  
434 Juan Aparicio Ojea, Eugen Solowjow, and Sergey Levine. Residual reinforcement learning for  
435 robot control. In *2019 International Conference on Robotics and Automation (ICRA)*, pages  
436 6023–6029. IEEE, 2019.
- 437 [20] Richard Cheng, Gábor Orosz, Richard M Murray, and Joel W Burdick. End-to-end safe  
438 reinforcement learning through barrier functions for safety-critical continuous control tasks. In  
439 *Proceedings of the AAAI conference on artificial intelligence*, volume 33, pages 3387–3395,  
440 2019.
- 441 [21] Hongpeng Cao, Yanbing Mao, Lui Sha, and Marco Caccamo. Physics-regulated deep reinforce-  
442 ment learning: Invariant embeddings. In *The Twelfth International Conference on Learning*  
443 *Representations*, 2024.
- 444 [22] Hongpeng Cao, Yanbing Mao, Lui Sha, and Marco Caccamo. Physics-model-regulated deep  
445 reinforcement learning towards safety & stability guarantees. In *62nd IEEE Conference on*  
446 *Decision and Control*, pages 8300–8305, 2023.
- 447 [23] Xue Bin Peng, Marcin Andrychowicz, Wojciech Zaremba, and Pieter Abbeel. Sim-to-real  
448 transfer of robotic control with dynamics randomization. In *2018 IEEE International Conference*  
449 *on Robotics and Automation (ICRA)*. IEEE, May 2018.
- 450 [24] Anusha Nagabandi, Ignasi Clavera, Simin Liu, Ronald S. Fearing, Pieter Abbeel, Sergey  
451 Levine, and Chelsea Finn. Learning to adapt in dynamic, real-world environments through  
452 meta-reinforcement learning, 2019.
- 453 [25] Jie Tan, Tingnan Zhang, Erwin Coumans, Atıl İscen, Yunfei Bai, Danijar Hafner, Steven Bohez,  
454 and Vincent Vanhoucke. Sim-to-real: Learning agile locomotion for quadruped robots. *Robotics:*  
455 *Science and Systems*, 2018.
- 456 [26] Wenhao Yu, Jie Tan, C Karen Liu, and Greg Turk. Preparing for the unknown: Learning a  
457 universal policy with online system identification. *Robotics: Science and Systems*, 2017.
- 458 [27] Hongpeng Cao, Mirco Theile, Federico G. Wyrwal, and Marco Caccamo. Cloud-edge training  
459 architecture for sim-to-real deep reinforcement learning. In *2022 IEEE/RSJ International*  
460 *Conference on Intelligent Robots and Systems (IROS)*, pages 9363–9370, 2022.
- 461 [28] Chieko Sarah Imai, Minghao Zhang, Yuchen Zhang, Marcin Kierebiński, Ruihan Yang, Yuzhe  
462 Qin, and Xiaolong Wang. Vision-guided quadrupedal locomotion in the wild with multi-modal  
463 delay randomization. In *2022 IEEE/RSJ international conference on intelligent robots and*  
464 *systems (IROS)*, pages 5556–5563. IEEE, 2022.
- 465 [29] Yuqing Du, Olivia Watkins, Trevor Darrell, Pieter Abbeel, and Deepak Pathak. Auto-tuned  
466 sim-to-real transfer, 2021.
- 467 [30] Quan Vuong, Sharad Vikram, Hao Su, Sicun Gao, and Henrik I. Christensen. How to pick the  
468 domain randomization parameters for sim-to-real transfer of reinforcement learning policies?,  
469 2019.
- 470 [31] Tsung-Yen Yang, Tingnan Zhang, Linda Luu, Sehoon Ha, Jie Tan, and Wenhao Yu. Safe  
471 reinforcement learning for legged locomotion. In *2022 IEEE/RSJ International Conference on*  
472 *Intelligent Robots and Systems (IROS)*, pages 2454–2461. IEEE, 2022.
- 473 [32] Fereshteh Sadeghi and Sergey Levine. Cad2rl: Real single-image flight without a single real  
474 image, 2017.
- 475 [33] Thomas Bartz-Beielstein. Why we need an AI-resilient society. *arXiv:1912.08786*, 2019.
- 476 [34] Rajesh Rajamani. *Vehicle dynamics and control*. Springer Science & Business Media, 2011.

- [35] Jan Roskam. *Airplane flight dynamics and automatic flight controls*. DARcorporation, 1995.
- [36] Lui Sha et al. Using simplicity to control complexity. *IEEE Software*, 18(4):20–28, 2001.
- [37] Stanley Bak, Taylor T Johnson, Marco Caccamo, and Lui Sha. Real-time reachability for verified Simplex design. In *2014 IEEE Real-Time Systems Symposium*, pages 138–148. IEEE, 2014.
- [38] Yanbing Mao, Yuliang Gu, Naira Hovakimyan, Lui Sha, and Petros Voulgaris.  $SL_1$ -simplex: Safe velocity regulation of self-driving vehicles in dynamic and unforeseen environments. *ACM Transactions on Cyber-Physical Systems*, 7(1):1–24, 2023.
- [39] Ruihan Yang, Minghao Zhang, Nicklas Hansen, Huazhe Xu, and Xiaolong Wang. Learning vision-guided quadrupedal locomotion end-to-end with cross-modal transformers. *2022 International Conference on Learning Representations*, 2022.
- [40] Siddhant Gangapurwala, Alexander Mitchell, and Ioannis Havoutis. Guided constrained policy optimization for dynamic quadrupedal robot locomotion. *IEEE Robotics and Automation Letters*, 5(2):3642–3649, 2020.
- [41] Timothy P. Lillicrap, Jonathan J. Hunt, Alexander Pritzel, Nicolas Heess, Tom Erez, Yuval Tassa, David Silver, and Daan Wierstra. Continuous control with deep reinforcement learning. In *4th International Conference on Learning Representations, ICLR*, 2016.
- [42] Tuomas Haarnoja, Aurick Zhou, Pieter Abbeel, and Sergey Levine. Soft actor-critic: Off-policy maximum entropy deep reinforcement learning with a stochastic actor. In Jennifer Dy and Andreas Krause, editors, *Proceedings of the 35th International Conference on Machine Learning*, volume 80 of *Proceedings of Machine Learning Research*, pages 1861–1870. PMLR, 10–15 Jul 2018.
- [43] Marcin Andrychowicz, Filip Wolski, Alex Ray, Jonas Schneider, Rachel Fong, Peter Welinder, Bob McGrew, Josh Tobin, OpenAI Pieter Abbeel, and Wojciech Zaremba. Hindsight experience replay. *Advances in neural information processing systems*, 30, 2017.
- [44] Khimya Khetarpal, Matthew Riemer, Irina Rish, and Doina Precup. Towards continual reinforcement learning: A review and perspectives. *Journal of Artificial Intelligence Research*, 75:1401–1476, 2022.
- [45] Scott Fujimoto, Herke Hoof, and David Meger. Addressing function approximation error in actor-critic methods. In *International conference on machine learning*, pages 1587–1596. PMLR, 2018.
- [46] Pascal Gahinet, Arkadii Nemirovskii, Alan J Laub, and Mahmoud Chilali. The lmi control toolbox. In *Proceedings of 1994 33rd IEEE conference on decision and control*, volume 3, pages 2038–2041. IEEE, 1994.
- [47] Stephen Boyd, Laurent El Ghaoui, Eric Feron, and Venkataramanan Balakrishnan. *Linear matrix inequalities in system and control theory*. SIAM, 1994.
- [48] Greg Brockman, Vicki Cheung, Ludwig Pettersson, Jonas Schneider, John Schulman, Jie Tang, and Wojciech Zaremba. OpenAI Gym, 2016.
- [49] Fuzhen Zhang. *The Schur complement and its applications*, volume 4. Springer Science & Business Media, 2006.
- [50] John Schulman, Filip Wolski, Prafulla Dhariwal, Alec Radford, and Oleg Klimov. Proximal policy optimization algorithms. *arXiv preprint <https://arxiv.org/abs/1707.06347>*.
- [51] Steven M Kay. *Fundamentals of statistical signal processing: estimation theory*. Prentice-Hall, Inc., 1993.
- [52] Răzvan Florian. Correct equations for the dynamics of the cart-pole system. 08 2005.
- [53] Michael Grant, Stephen Boyd, and Yinyu Ye. Cvx users’ guide. online: <http://www.stanford.edu/boyd/software.html>, 2009.

- 524 [54] Lieven Vandenbergh, Stephen Boyd, and Shao-Po Wu. Determinant maximization with linear  
525 matrix inequality constraints. *SIAM journal on matrix analysis and applications*, 19(2):499–533,  
526 1998.
- 527 [55] Yuxiang Yang. Github: Quadruped robot simulator.
- 528 [56] Jared Di Carlo, Patrick M Wensing, Benjamin Katz, Gerardo Bledt, and Sangbae Kim. Dynamic  
529 locomotion in the mit cheetah 3 through convex model-predictive control. In *2018 IEEE/RSJ*  
530 *international conference on intelligent robots and systems (IROS)*, pages 1–9. IEEE, 2018.

# 531 Appendices

532	<b>A</b>	<b>Notations throughout Paper</b>	<b>15</b>
533	<b>B</b>	<b>Auxiliary Lemmas</b>	<b>16</b>
534	<b>C</b>	<b>Control Contribution Ratio</b>	<b>17</b>
535	<b>D</b>	<b>Proof Theorem C.1</b>	<b>19</b>
536	<b>E</b>	<b>Least-square Regression Based System Identification for Obtaining Model Knowledge</b>	<b>21</b>
537	<b>F</b>	<b>Experiment: Cart-Pole System</b>	<b>22</b>
538	<b>G</b>	<b>Experiment: Real Quadruped Robot</b>	<b>25</b>
539	<b>H</b>	<b>Computation Resources</b>	<b>29</b>

## 540 **A Notations throughout Paper**

### 541 **A.1 Notations**

Table 1: Notations throughout Paper

$\mathbb{R}^n$	set of $n$ -dimensional real vectors
$\mathbb{N}$	set of natural numbers
$\mathbf{x}_i$	$i$ -th entry of vector $\mathbf{x}$
$\mathbf{W}_{i,:}$	$i$ -th row of matrix $\mathbf{W}$
$\mathbf{W}_{i,j}$	matrix $\mathbf{W}$ 's element at row $i$ and column $j$
$\mathbf{P} \succ (\prec) 0$	matrix $\mathbf{P}$ is positive (negative) definite
$\top$	matrix or vector transposition
$ \cdot $	set cardinality, or absolute value
$\mathbf{I}_n$	$n$ -dimensional identity matrix
$\mathbf{O}_{m \times n}$	$m \times n$ -dimensional zero matrix
$\mathbb{X} \setminus \Omega$	complement set of $\Omega$ with respect to $\mathbb{X}$



## 542 B Auxiliary Lemmas

543 **Lemma B.1** (Schur Complement [49]). *For any symmetric matrix  $\mathbf{M} = \begin{bmatrix} \mathbf{A} & \mathbf{B} \\ \mathbf{B}^\top & \mathbf{C} \end{bmatrix}$ , then  $\mathbf{M} \succ 0$  if*  
 544 *and only if  $\mathbf{C} \succ 0$  and  $\mathbf{A} - \mathbf{B}\mathbf{C}^{-1}\mathbf{B}^\top \succ 0$ .*

545 **Lemma B.2.** [21] *Consider the sets defined in Equation (2) and Equation (3). We have  $\Omega \subseteq \mathbb{X}$ , if*

$$[\underline{\mathbf{D}}]_{i,:} \cdot \mathbf{P}^{-1} \cdot [\underline{\mathbf{D}}]_{:,i}^\top = \begin{cases} \geq 1, & [\mathbf{d}]_i = 1 \\ \leq 1, & [\mathbf{d}]_i = -1 \end{cases}, \quad [\overline{\mathbf{D}}]_{i,:} \cdot \mathbf{P}^{-1} \cdot [\overline{\mathbf{D}}]_{:,i}^\top \leq 1, \quad i \in \{1, \dots, h\}, \quad (24)$$

546 *where  $\overline{\mathbf{D}} = \frac{\mathbf{D}}{\underline{\Lambda}}$ ,  $\underline{\mathbf{D}} = \frac{\mathbf{D}}{\underline{\Lambda}}$ , and for  $i, j \in \{1, \dots, h\}$ ,*

$$[\mathbf{d}]_i \triangleq \begin{cases} 1, & [\underline{\mathbf{v}} + \mathbf{v}]_i > 0 \\ 1, & [\overline{\mathbf{v}} + \mathbf{v}]_i < 0, \\ -1, & \text{otherwise} \end{cases}, \quad [\overline{\Lambda}]_{i,j} \triangleq \begin{cases} 0, & i \neq j \\ [\overline{\mathbf{v}} + \mathbf{v}]_i, & [\underline{\mathbf{v}} + \mathbf{v}]_i > 0 \\ [\underline{\mathbf{v}} + \mathbf{v}]_i, & [\overline{\mathbf{v}} + \mathbf{v}]_i < 0 \\ [\overline{\mathbf{v}} + \mathbf{v}]_i, & \text{otherwise} \end{cases}, \quad [\underline{\Lambda}]_{i,j} \triangleq \begin{cases} 0, & i \neq j \\ [\underline{\mathbf{v}} + \mathbf{v}]_i, & [\underline{\mathbf{v}} + \mathbf{v}]_i > 0 \\ [\overline{\mathbf{v}} + \mathbf{v}]_i, & [\overline{\mathbf{v}} + \mathbf{v}]_i < 0 \\ [-\underline{\mathbf{v}} - \mathbf{v}]_i, & \text{otherwise} \end{cases}.$$

547

548 **Lemma B.3.** *Consider the action set  $\mathbb{A}_{\text{phy}}$  defined in Equation (7), and*

$$\Phi \triangleq \{ \mathbf{a} \in \mathbb{R}^m \mid \mathbf{a}^\top \cdot \mathbf{V} \cdot \mathbf{a} \leq 1, \mathbf{V} \succ 0 \}. \quad (25)$$

549 *We have  $\Phi \subseteq \mathbb{A}_{\text{phy}}$ , if*

$$[\overline{\mathbf{C}}]_{i,:} \cdot \mathbf{V}^{-1} \cdot [\overline{\mathbf{C}}]_{:,i}^\top \leq 1, \quad [\underline{\mathbf{C}}]_{i,:} \cdot \mathbf{V}^{-1} \cdot [\underline{\mathbf{C}}]_{:,i}^\top = \begin{cases} \geq 1, & \text{if } [\mathbf{c}]_i = 1 \\ \leq 1, & \text{if } [\mathbf{c}]_i = -1 \end{cases}, \quad i \in \{1, \dots, g\} \quad (26)$$

550 *where  $\overline{\mathbf{C}} = \frac{\mathbf{C}}{\underline{\Delta}}$ ,  $\underline{\mathbf{C}} = \frac{\mathbf{C}}{\underline{\Delta}}$ , and for  $i, j \in \{1, \dots, g\}$ ,*

$$[\mathbf{c}]_i \triangleq \begin{cases} 1, & [\underline{\mathbf{z}} + \mathbf{z}]_i > 0 \\ 1, & [\overline{\mathbf{z}} + \mathbf{z}]_i < 0, \\ -1, & \text{otherwise} \end{cases}, \quad [\overline{\Delta}]_{i,j} \triangleq \begin{cases} 0, & i \neq j \\ [\overline{\mathbf{z}} + \mathbf{z}]_i, & [\underline{\mathbf{z}} + \mathbf{z}]_i > 0 \\ [\underline{\mathbf{z}} + \mathbf{z}]_i, & [\overline{\mathbf{z}} + \mathbf{z}]_i < 0 \\ [\overline{\mathbf{z}} + \mathbf{z}]_i, & \text{otherwise} \end{cases}, \quad [\underline{\Delta}]_{i,j} \triangleq \begin{cases} 0, & i \neq j \\ [\underline{\mathbf{z}} + \mathbf{z}]_i, & [\underline{\mathbf{z}} + \mathbf{z}]_i > 0 \\ [\overline{\mathbf{z}} + \mathbf{z}]_i, & [\overline{\mathbf{z}} + \mathbf{z}]_i < 0 \\ [-\underline{\mathbf{z}} - \mathbf{z}]_i, & \text{otherwise} \end{cases}.$$

551

552 *Proof.* The proof path of Lemma B.3 is the same as that of Lemma B.2 in [21]. So, it is omitted  
 553 here.  $\square$

## C Control Contribution Ratio

### C.1 Controllable Data-driven Action Space

In continuous control tasks, actions of the data-driven approaches are typically generated by policies parameterized with deep neural networks, which map states to actions. In DRL, deterministic policies, as described in DDPG [41], directly map states to actions within the interval  $[-1, 1]$  using the Tanh activation function at the output layer. On the other hand, stochastic policies, such as those proposed in the Soft Actor-Critic (SAC)[42] algorithm and Proximal Policy Optimization (PPO) [50], sample actions from a learned Gaussian distribution with reparameterization trick, followed by Tanh activation to ensure actions remain within the  $[-1, 1]$  interval. To adapt the generated action for actual control commands, the action is rescaled by a magnitude factor  $M_l$ , expanding the action space to  $[-M_l, M_l]$ . This allows for the flexible adaptation of the action space to the specific requirements of different control tasks.

### C.2 Controllable Physics-model-based Action Space

The controllable physics-model-based action space is delivered by incorporating two additional conditions (26) and (28) into Theorem 5.3's LMIs in [21]. The updated version is formally stated in the following theorem.

**Theorem C.1.** *Consider the system (1) under control of Phy-DRL, consisting of residual policy (4) and safety-embedded reward (5), wherein matrices  $\mathbf{F}$  and  $\mathbf{P}$  are computed according to*

$$\mathbf{F} = \mathbf{R} \cdot \mathbf{Q}^{-1}, \quad \mathbf{P} = \mathbf{Q}^{-1}, \quad (27)$$

and  $\mathbf{R}$  and  $\mathbf{Q}^{-1}$  satisfying the inequalities (24), (26) with  $\mathbf{V} = \beta \cdot \mathbf{I}_m \succ 0$ , and

$$\begin{bmatrix} \mathbf{Q} & \mathbf{R}^\top \\ \mathbf{R} & \frac{1}{\beta} \cdot \mathbf{I}_m \end{bmatrix} \succ 0, \quad (28)$$

$$\begin{bmatrix} \alpha \cdot \mathbf{Q} & \mathbf{Q} \cdot \mathbf{A}^\top + \mathbf{R}^\top \cdot \mathbf{B}^\top \\ \mathbf{A} \cdot \mathbf{Q} + \mathbf{B} \cdot \mathbf{R} & \mathbf{Q} \end{bmatrix} \succ 0, \quad \text{with a given } \alpha \in (0, 1). \quad (29)$$

With the sets  $\Omega$  (3),  $\mathbb{X}$  (2),  $\mathbb{A}$  (7), and  $\Phi$  (25) at hand, the system (1) has the following properties:

1. Given any  $\mathbf{s}(1) \in \Omega$ , the system state  $\mathbf{s}(k) \in \Omega \subseteq \mathbb{X}$  holds for any  $k \in \mathbb{N}$  (i.e., the safety of system (1) is guaranteed), if the sub-reward  $r(\mathbf{s}(k), \mathbf{s}(k+1))$  in Equation (5) satisfies  $r(\mathbf{s}(k), \mathbf{s}(k+1)) \geq \alpha - 1, \forall k \in \mathbb{N}$ .
2. If the state  $\mathbf{s}(k) \in \Omega \subseteq \mathbb{X}$ , the physics-model-based control command in Equation (4) satisfies  $\mathbf{a}_{\text{phy}}(k) \in \Phi \subseteq \mathbb{A}_{\text{phy}}$ .

*Proof.* Item 1 is a direct result of Theorem 5.3 in [21], which is not influenced by the additional conditions (28) and Equation (26). So, its proof is omitted.

We now focus on the proof of Item 2 of Theorem C.1. Since  $\beta > 0$  and  $\mathbf{V} = \beta \cdot \mathbf{I}_m$ , according to Lemma B.1, the condition (28) implies that

$$\mathbf{Q} - \beta \cdot \mathbf{R}^\top \cdot \mathbf{R} = \mathbf{Q} - \mathbf{R}^\top \cdot \mathbf{V} \cdot \mathbf{R} \succ 0. \quad (30)$$

Substituting  $\mathbf{F} \cdot \mathbf{Q} = \mathbf{R}_i$  into (30) leads to  $\mathbf{Q} - (\mathbf{F} \cdot \mathbf{Q})^\top \cdot \mathbf{V} \cdot (\mathbf{F} \cdot \mathbf{Q}) \succ 0$ , multiplying both left-hand and right-hand sides of which by  $\mathbf{Q}^{-1}$  yields  $\mathbf{Q}^{-1} - \mathbf{F}^\top \cdot \mathbf{V} \cdot \mathbf{F} \succ 0$ . We thus have

$$\mathbf{s}^\top(k) \cdot \mathbf{Q}^{-1} \cdot \mathbf{s}(k) - \mathbf{s}^\top(k) \cdot \mathbf{F}^\top \cdot \mathbf{V} \cdot \mathbf{F} \cdot \mathbf{s}(k) = \mathbf{s}^\top(k) \cdot \mathbf{P} \cdot \mathbf{s}(k) - \mathbf{a}_{\text{phy}}^\top(k) \cdot \mathbf{V} \cdot \mathbf{a}_{\text{phy}}(k) > 0,$$

which is obtained via considering  $\mathbf{P} = \mathbf{Q}^{-1}$  and  $\mathbf{F} = \mathbf{R} \cdot \mathbf{Q}^{-1} = \mathbf{R} \cdot \mathbf{P}$ . The inequality means  $\mathbf{s}^\top(k) \cdot \mathbf{P} \cdot \mathbf{s}(k) > \mathbf{a}_{\text{phy}}^\top(k) \cdot \mathbf{V} \cdot \mathbf{a}_{\text{phy}}(k)$ . Therefore, in light of the definition of safety envelope (3), we conclude that if  $\mathbf{s}(k) \in \Omega$ , i.e.,  $\mathbf{s}^\top(k) \cdot \mathbf{P} \cdot \mathbf{s}(k) < 1$ , then  $\mathbf{a}_{\text{phy}}^\top(k) \cdot \mathbf{V} \cdot \mathbf{a}_{\text{phy}}(k) < 1$ . Furthermore, considering (26) in Lemma B.3 in conjunction with defined set (25), we conclude  $\mathbf{a}_{\text{phy}}(k) \in \Phi \subseteq \mathbb{A}$ , which completes the proof.  $\square$

### 590 C.3 Automatic Constructions of Residual Action Policy and Safety-embedded Reward

591 Given the matrices  $\mathbf{F}$  and  $\mathbf{P}$ , the residual policy Equation (4) and safety-embedded reward Equation (5)  
 592 are delivered immediately. With the available physics-model knowledge  $(\mathbf{A}, \mathbf{B})$  at hand, the  $\mathbf{F}$  and  
 593  $\mathbf{P}$  can be automatically computed from LMIs in Equation (24), Equation (26), Equation (28), and  
 594 Equation (29), by LMI toolbox [46, 47].

595 We can also find optimal  $\mathbf{R}$  and  $\mathbf{Q}$  that can maximize the safety envelope. To achieve this, we recall  
 596 the volume of a safety envelope (3) is proportional to  $\sqrt{\det(\mathbf{P}^{-1})}$ , the interested problem is thus a  
 597 typical analytic centering problem, formulated as given a  $\alpha \in (0, 1)$ ,

$$\underset{\mathbf{Q}, \mathbf{R}}{\operatorname{argmin}} \{ \log \det(\mathbf{Q}^{-1}) \} = \underset{\mathbf{Q}, \mathbf{R}}{\operatorname{argmin}} \{ \log \det(\mathbf{P}^{-1}) \}, \text{ subject to LMIs (24), (26), (28), (29).}$$

## 598 **D Proof Theorem C.1**

### 599 **Proof of Item 1**

600 We define a Lyapunov candidate for a real plant described in Equation (13):

$$V(k) = \mathbf{e}^\top(k) \cdot \hat{\mathbf{P}} \cdot \mathbf{e}(k), \quad (31)$$

601 which along the dynamics (13), in conjunction with the action policy (14), results in

$$\begin{aligned} & V(k+1) - \beta \cdot V(k) \\ &= \mathbf{e}^\top(k+1) \cdot \hat{\mathbf{P}} \cdot \mathbf{e}(k+1) - \beta \cdot \mathbf{e}^\top(k) \cdot \hat{\mathbf{P}} \cdot \mathbf{e}(k) \\ &= \mathbf{e}^\top(k) \cdot \left( \bar{\mathbf{A}}^\top(s(k)) \cdot \hat{\mathbf{P}} \cdot \bar{\mathbf{A}}(s(k)) - \beta \cdot \hat{\mathbf{P}} \right) \cdot \mathbf{e}(k) + \mathbf{h}^\top(\mathbf{e}(k)) \cdot \hat{\mathbf{P}} \cdot \mathbf{h}(\mathbf{e}(k)) \\ &\quad + 2\mathbf{e}^\top(k) \cdot \left( \bar{\mathbf{A}}(s(k)) \cdot \hat{\mathbf{P}} \right) \cdot \mathbf{h}(\mathbf{e}(k)), \end{aligned} \quad (32)$$

602 where we define:

$$\bar{\mathbf{A}}(s(k)) \triangleq \mathbf{A}(s(k)) + \mathbf{B}(s(k)) \cdot \hat{\mathbf{F}}. \quad (33)$$

603 It is straightforward to verify the inequality

$$\begin{aligned} & 2\mathbf{e}^\top(k) \cdot \left( \bar{\mathbf{A}}(s(k)) \cdot \hat{\mathbf{P}} \right) \cdot \mathbf{h}(\mathbf{e}(k)) \\ & \leq \omega \cdot \mathbf{e}^\top(k) \cdot \bar{\mathbf{A}}^\top(s(k)) \cdot \hat{\mathbf{P}} \cdot \bar{\mathbf{A}}(s(k)) \cdot \mathbf{e}(k) + \frac{1}{\omega} \cdot \mathbf{h}^\top(\mathbf{e}(k)) \cdot \hat{\mathbf{P}} \cdot \mathbf{h}(\mathbf{e}(k)), \end{aligned} \quad (34)$$

604 holds for any  $\omega > 0$ .

605 Meanwhile, noting  $\hat{\mathbf{Q}} = \hat{\mathbf{P}}^{-1}$ , the inequality in Equation (17) is equivalent to  $\eta \cdot \mathbf{P} \succ \hat{\mathbf{P}} \succ \mathbf{P}$ , which  
606 in light of Assumption 6.1 then results in

$$\begin{aligned} \mathbf{h}^\top(\mathbf{e}(k)) \cdot \hat{\mathbf{P}} \cdot \mathbf{h}(\mathbf{e}(k)) & \leq \mathbf{h}^\top(\mathbf{e}(k)) \cdot \eta \cdot \mathbf{P} \cdot \mathbf{h}(\mathbf{e}(k)) \leq \mathbf{e}^\top(k) \cdot \kappa \cdot \eta \cdot \mathbf{P} \cdot \mathbf{e}(k) \\ & \leq \mathbf{e}^\top(k) \cdot \kappa \cdot \eta \cdot \hat{\mathbf{P}} \cdot \mathbf{e}(k). \end{aligned} \quad (35)$$

607 Substituting inequalities in Equation (34) and Equation (35) into Equation (32) yields

$$\begin{aligned} & V(k+1) - \beta \cdot V(k) \\ & \leq \mathbf{e}^\top(k) \cdot \left( (1 + \omega) \cdot \bar{\mathbf{A}}^\top(s(k)) \cdot \hat{\mathbf{P}} \cdot \bar{\mathbf{A}}(s(k)) - (\beta - \kappa \cdot \eta \cdot (1 + \frac{1}{\omega})) \cdot \hat{\mathbf{P}} \right) \cdot \mathbf{e}(k). \end{aligned} \quad (36)$$

608 Recalling Schur Complement in Lemma B.1 in Appendix B and considering  $\hat{\mathbf{P}} \succ 0$ , we conclude  
609 that the inequality in Equation (18) is equivalent to

$$\begin{aligned} & (\beta - \kappa \cdot \eta \cdot (1 + \frac{1}{\omega})) \cdot \hat{\mathbf{Q}} \\ & - (1 + \omega) \cdot (\hat{\mathbf{Q}} \cdot \mathbf{A}^\top(s(k)) + \hat{\mathbf{R}}^\top \cdot \mathbf{B}^\top(s(k))) \cdot \hat{\mathbf{Q}}^{-1} \cdot (\mathbf{A}(s(k)) \cdot \hat{\mathbf{Q}} + \mathbf{B}(s(k)) \cdot \hat{\mathbf{R}}) \succ 0. \end{aligned} \quad (37)$$

610 Multiplying both the left-hand side and the right-hand side of inequality (37) by  $\hat{\mathbf{Q}}^{-1}$  yields

$$\begin{aligned} & (\beta - \kappa \cdot \eta \cdot (1 + \frac{1}{\omega})) \cdot \hat{\mathbf{Q}}^{-1} \\ & - (1 + \omega) \cdot (\mathbf{A}^\top(s(k)) + \hat{\mathbf{Q}}^{-1} \cdot \hat{\mathbf{R}}^\top \cdot \mathbf{B}^\top(s(k))) \cdot \hat{\mathbf{Q}}^{-1} \cdot (\mathbf{A}(s(k)) + \mathbf{B}(s(k)) \cdot \hat{\mathbf{R}} \cdot \mathbf{Q}^{-1}) \succ 0, \end{aligned}$$

611 substituting the definitions in Equation (16) into which leads to

$$\begin{aligned} & (\beta - \kappa \cdot \eta \cdot (1 + \frac{1}{\omega})) \cdot \hat{\mathbf{P}} \\ & - (1 + \omega) \cdot (\mathbf{A}^\top(s(k)) + \hat{\mathbf{F}}^\top \cdot \mathbf{B}^\top(s(k))) \cdot \hat{\mathbf{P}} \cdot (\mathbf{A}(s(k)) + \mathbf{B}(s(k)) \cdot \hat{\mathbf{F}}) \succ 0. \end{aligned} \quad (38)$$

612 Recalling (33), the inequality in Equation (38) is equivalent to

$$(1 + \omega) \cdot \bar{\mathbf{A}}^\top(s(k)) \cdot \hat{\mathbf{P}} \cdot \bar{\mathbf{A}}(s(k)) - (\beta - \kappa \cdot \eta \cdot (1 + \frac{1}{\omega})) \cdot \hat{\mathbf{P}} \prec 0,$$

613 which, in conjunction with Equation (36), leads to  $V(k+1) - \beta \cdot V(k) \leq 0$ , i.e.,  $V(k+1) \leq$   
614  $\beta \cdot V(k)$ , we thus complete the proof of Item 1.

615 **Proof of Item 2**

616 For patch envelope (15), we introduce its boundary:

$$\partial\Omega_{\text{patch}} \triangleq \left\{ \mathbf{x} \mid (\mathbf{x} - \bar{\mathbf{s}}^*)^\top \cdot \hat{\mathbf{P}} \cdot (\mathbf{x} - \bar{\mathbf{s}}^*) = (1 - \chi)^2 \cdot \mathbf{s}^\top(k) \cdot \hat{\mathbf{P}} \cdot \mathbf{s}(k), \hat{\mathbf{P}} \succ 0 \right\},$$

617 which, in light of  $\mathbf{e} \triangleq \mathbf{x} - \bar{\mathbf{s}}^*$ , is equivalent to

$$\partial\Omega_{\text{patch}} \triangleq \left\{ \mathbf{x} \mid \mathbf{e}^\top \cdot \hat{\mathbf{P}} \cdot \mathbf{e} = (1 - \chi)^2 \cdot \mathbf{s}^\top(k) \cdot \hat{\mathbf{P}} \cdot \mathbf{s}(k) \right\}, \quad (39)$$

618 by which, the proof of  $\Omega_{\text{patch}} \subseteq \Omega$  equivalently transforms to the proof of  $\partial\Omega_{\text{patch}} \subseteq \Omega$ .

619 To move forward, we first recall  $\hat{\mathbf{P}} = \hat{\mathbf{Q}}^{-1} \succ 0$ , in light of which, the inequality in Equation (17) is  
620 equivalent to

$$\mathbf{P} \prec \hat{\mathbf{P}} \prec \eta \cdot \mathbf{P}, \quad \text{with } \eta > 1. \quad (40)$$

621 Meanwhile, recalling  $\mathbf{e} = \mathbf{x} - \chi \cdot \mathbf{s}^*$ , and we define

$$\mathbf{e}^* = \mathbf{x}^* - \chi \cdot \mathbf{s}(k) = \mathbf{s}(k) - \chi \cdot \mathbf{s}(k) = (1 - \chi) \cdot \mathbf{s}(k), \quad (41)$$

622 considering which, for any  $\mathbf{x} \in \partial\Omega_{\text{patch}}$ , it is straightforward to verify that

$$\begin{aligned} \mathbf{x}^\top \cdot \mathbf{P} \cdot \mathbf{x} &= (\mathbf{e} + \chi \cdot \mathbf{s}(k))^\top \cdot \mathbf{P} \cdot (\mathbf{e} + \chi \cdot \mathbf{s}(k)) \\ &= \mathbf{e}^\top \cdot \mathbf{P} \cdot \mathbf{e} + \chi^2 \cdot \mathbf{s}^\top(k) \cdot \mathbf{P} \cdot \mathbf{s}(k) + 2\chi \cdot \mathbf{e}^\top \cdot \mathbf{P} \cdot \mathbf{s}(k) \\ &\leq 2 \cdot \mathbf{e}^\top \cdot \mathbf{P} \cdot \mathbf{e} + 2\chi^2 \cdot \mathbf{s}^\top(k) \cdot \mathbf{P} \cdot \mathbf{s}(k) \end{aligned} \quad (42)$$

$$\leq 2 \cdot \mathbf{e}^\top \cdot \mathbf{P} \cdot \mathbf{e} + 2\chi^2 \cdot \varepsilon \quad (43)$$

$$\leq 2 \cdot \mathbf{e}^\top \cdot \hat{\mathbf{P}} \cdot \mathbf{e} + 2\chi^2 \cdot \varepsilon \quad (44)$$

$$= 2 \cdot (1 - \chi)^2 \cdot \mathbf{s}^\top(k) \cdot \hat{\mathbf{P}} \cdot \mathbf{s}(k) + 2\chi^2 \cdot \varepsilon \quad (45)$$

$$= 2 \cdot \eta \cdot (1 - \chi)^2 \cdot \mathbf{s}^\top(k) \cdot \mathbf{P} \cdot \mathbf{s}(k) + 2\chi^2 \cdot \varepsilon \quad (46)$$

$$= 2 \cdot \eta \cdot (1 - \chi)^2 \cdot \varepsilon + 2\chi^2 \cdot \varepsilon \quad (47)$$

623 We note Equation (42) is obtained from its previous step via considering the well-known inequality:  
624  $2\chi \cdot \mathbf{e}^\top \cdot \mathbf{P} \cdot \mathbf{s}(k) \leq \mathbf{s}^\top(k) \cdot \mathbf{P} \cdot \mathbf{s}(k) + \chi^2 \cdot \mathbf{e}^\top \cdot \mathbf{P} \cdot \mathbf{e}$ . We let  $\mathbf{x}^* = \mathbf{s}(k)$  be a state sample of  
625 triggering condition for guaranteeing  $\mathbf{s}^\top(k) \cdot \mathbf{P} \cdot \mathbf{s}(k) \leq \varepsilon$ , which is the root that derives Equation (43)  
626 from Equation (42). Equation (44) from Equation (43) is obtained via considering the left-hand side  
627 inequality in Equation (40). Equation (45) from Equation (44) is obtained in light of Equation (39)  
628 and the fact  $\mathbf{s} \in \partial\Omega_{\text{patch}}$ . Equation (46) from Equation (45) is obtained via considering right-hand  
629 side inequality in Equation (40). Lastly, Equation (47) is obtained from Equation (46) by considering  
630 the fact that the  $\mathbf{x}^* = \mathbf{s}(k)$  is a state sample inside safety envelope, so satisfying  $\mathbf{s}^\top(k) \cdot \mathbf{P} \cdot \mathbf{s}(k) \leq 1$ .

631 Recall that the inequality in Equation (19) is equivalent to  $2\eta \cdot (1 - \chi)^2 \cdot \varepsilon + 2\chi^2 \cdot \varepsilon \leq 1$ , which, in  
632 conjunction with Equation (47), leads to the conclusion that for any  $\mathbf{x} \in \partial\Omega_{\text{patch}}$ ,  $\mathbf{x}^\top \cdot \hat{\mathbf{P}} \cdot \mathbf{x} \leq 1$  holds.  
633 In other words, in light of Equation (3), for any  $\mathbf{x} \in \partial\Omega_{\text{patch}}$ , the  $\mathbf{x} \in \Omega$  holds. We thus conclude  
634  $\partial\Omega_{\text{patch}} \subseteq \Omega$ , which completes the proof.

## E Least-square Regression Based System Identification for Obtaining Model Knowledge

This section considers the extreme case that in practice, the user has zero knowledge about  $(\mathbf{A}(\mathbf{s}(k)), \mathbf{B}(\mathbf{s}(k)))$ . To timely obtain  $(\mathbf{A}(\mathbf{s}(k)), \mathbf{B}(\mathbf{s}(k)))$ , we consider the approach of system identification, which is based on least-square regression, using only a few most recent sensor data. To formulate the approach, we assume the ground-truth dynamics of CPS with noisy outputs can be described by

$$\begin{aligned} \text{System dynamics:} \quad & \mathbf{s}(k+1) = \mathbf{A}(\mathbf{s}(k)) \cdot \mathbf{s}(k) + \mathbf{B}(\mathbf{s}(k)) \cdot \mathbf{u}(k) + p(k), \\ \text{Noisy system-state sampling:} \quad & \mathbf{y}(k) = \mathbf{s}(k) + o_x(k), \\ \text{Noisy control-command sampling:} \quad & \mathbf{a}(k) = \mathbf{u}(k) + o_u(k), \end{aligned}$$

where  $\mathbf{A}(\mathbf{s}(k))$ ,  $\mathbf{B}(\mathbf{s}(k))$ ,  $\mathbf{s}(k)$ ,  $\mathbf{u}(k)$ ,  $\mathbf{y}(k)$ ,  $\mathbf{a}(k)$ ,  $p(k)$ ,  $o_x(k)$  and  $o_u(k)$  denote the system matrix, control structure matrix, noise-free system state, noise-free control command, noisy system-state sampling, noisy control-command sampling, model mismatch, noise of system-state sampling, and noise of control-command sampling, respectively.

The proposed system identification is to use only a few (most recently generated) noisy samplings of system states and control commands to learn the system model, represented by the block matrix  $[\mathbf{A}(\mathbf{s}(k)), \mathbf{B}(\mathbf{s}(k))]$ , being subject to available physics knowledge. The system model  $[\mathbf{A}(\mathbf{s}(k)), \mathbf{B}(\mathbf{s}(k))]$  will be obtained by solving the following regression problem:

$$[\hat{\mathbf{A}}(\mathbf{s}(k)), \hat{\mathbf{B}}(\mathbf{s}(k))] = \arg \min_{[\mathbf{A}(\mathbf{s}(k)), \mathbf{B}(\mathbf{s}(k))]} \{ \|\mathbf{Y}(k, \tau) - [\mathbf{A}(\mathbf{s}(k)), \mathbf{B}(\mathbf{s}(k))] \cdot \mathfrak{M}(k, \tau)\|_2 \}, \quad (48)$$

where the  $\mathbf{Y}(k, \tau)$  and  $\mathfrak{M}(k, \tau)$  are formed by  $\tau \in \mathbb{N}$  sensor samplings, i.e.,

$$\begin{aligned} \mathbf{Y}(k, \tau) &= [\mathbf{y}(k+1), \mathbf{y}(k+2), \dots, \mathbf{y}(k+\tau)], \\ \mathfrak{M}(k, \tau) &= \left[ \begin{bmatrix} \mathbf{y}(k) \\ \mathbf{u}(k) \end{bmatrix}, \begin{bmatrix} \mathbf{y}(k+1) \\ \mathbf{u}(k+1) \end{bmatrix}, \dots, \begin{bmatrix} \mathbf{y}(k+\tau-1) \\ \mathbf{u}(k+\tau-1) \end{bmatrix} \right]. \end{aligned}$$

Then, according to the reference [51], the optimal (least-square) solution of the problem (48) is

$$[\hat{\mathbf{A}}(\mathbf{s}(k)), \hat{\mathbf{B}}(\mathbf{s}(k))]^* = (\mathbf{Y}(k, \tau) \cdot \mathfrak{M}^\top(k, \tau)) \cdot (\mathfrak{M}(k, \tau) \cdot \mathfrak{M}^\top(k, \tau))^{-1},$$

which is our estimated model knowledge  $[\mathbf{A}(\mathbf{s}(k)), \mathbf{B}(\mathbf{s}(k))]$ .

## F Experiment: Cart-Pole System

### F.1 Pre-training and Continual Learning

We leverage the DDPG algorithm [41] to pre-train HP-Student, i.e., Phy-DRL, and support its continual learning. The actor and critic networks are implemented as a Multi-Layer Perceptron (MLP) with four fully connected layers. The output dimensions of critic and actor networks are 256, 128, 64, and 1, respectively. The activation functions of the first three neural layers are ReLU, while the output of the last layer is the Tanh function for the actor-network and Linear for the critic network. The input of the critic network is  $[s; a]$ , while the input of the actor-network is  $s$ . In more detail, we let discount factor  $\gamma = 0.9$ , and the learning rates of critic and actor networks are the same as 0.0003. We set the batch size to 200. The maximum step number of one episode is 500.

### F.2 System Dynamics

The physics knowledge about the dynamics of cart-pole systems used by HP-Student and HA-Teacher for their designs is from the following dynamics model in [52]:

$$\ddot{\theta} = \frac{g \sin \theta + \cos \theta \left( \frac{-F - m_p l \dot{\theta}^2 \sin \theta}{m_c + m_p} \right)}{l \left( \frac{4}{3} - \frac{m_p \cos^2 \theta}{m_c + m_p} \right)}, \quad (49a)$$

$$\ddot{x} = \frac{F + m_p l \left( \dot{\theta}^2 \sin \theta - \ddot{\theta} \cos \theta \right)}{m_c + m_p}, \quad (49b)$$

whose parameters' physical representations and values are given in Table 2.

Notation		Value	Unit
$m_c$	mass of cart	0.94	$kg$
$m_p$	mass of pole	0.23	$kg$
$g$	gravitational acceleration	9.8	$m \cdot s^{-2}$
$l$	half length of pole	0.32	$m$
$T$	sample period	1/30	$s$
$F$	actuator input	$[-30, 30]$	$N$
$\mu_c$	cart friction coefficient	18	
$\mu_p$	pole friction coefficient	0.0031	
$x$	position of cart	$[-0.8, 0.8]$	$m$
$\dot{x}$	velocity of cart	$[-3, 3]$	$m \cdot s^{-1}$
$\theta$	angle of pole	$[-0.9, 0.9]$	$rad$
$\dot{\theta}$	angular velocity of pole	$[-4.5, 4.5]$	$rad \cdot s^{-1}$

Table 2: Notation Table for Cart-Pole System

### F.3 HP-Student: Physics Knowledge and Design

As Phy-DRL allows us to simply have nonlinear dynamics (49) to an analyzable line model:

$$\dot{s} = \hat{\mathbf{A}} \cdot s + \hat{\mathbf{B}} \cdot a, \quad (50)$$

where  $s = [x, v, \theta, \omega]^\top$ . To have  $\hat{\mathbf{A}}$  and  $\hat{\mathbf{B}}$  from Equation (49), we let  $\cos \theta \approx 1$ ,  $\sin \theta \approx \theta$  and  $\omega^2 \sin \theta \approx 0$ . Meanwhile, the sampling technique transforms the continuous-time model (50) to the discrete-time model:

$$s(k+1) = \mathbf{A} \cdot s(k) + \mathbf{B} \cdot a(k), \text{ with } \mathbf{A} = \mathbf{I}_4 + T \cdot \hat{\mathbf{A}}, \mathbf{B} = T \cdot \hat{\mathbf{B}},$$

where we have

$$\mathbf{A} = \begin{bmatrix} 1 & 0.0333 & 0 & 0 \\ 0 & 1 & -0.0565 & 0 \\ 0 & 0 & 1 & 0.0333 \\ 0 & 0 & 0.8980 & 1 \end{bmatrix}, \quad \mathbf{B} = [0 \ 0.0334 \ 0 \ -0.0783]^\top. \quad (51)$$



673 Considering the safety conditions in Equation (22) and action space condition in Equation (23) and  
 674 the formulas of safety set in Equation (2) and action set in Equation (7), we have

$$\mathbf{D} = \begin{bmatrix} 1 & 0 & 0 & 0 \\ 0 & 0 & 1 & 0 \end{bmatrix}, \mathbf{v} = \begin{bmatrix} 0 \\ 0 \end{bmatrix}, \bar{\mathbf{v}} = \begin{bmatrix} 0.9 \\ 0.8 \end{bmatrix}, \underline{\mathbf{v}} = \begin{bmatrix} -0.9 \\ -0.8 \end{bmatrix}, \mathbf{C} = 1, \mathbf{z} = 0, \bar{\mathbf{z}} = 25, \underline{\mathbf{z}} = -25 \quad (52)$$

675 based on which, then according to the  $\bar{\Lambda}$ ,  $\underline{\Lambda}$  and  $\mathbf{d}$  defined in Lemma B.2,  $\bar{\Delta}$ ,  $\underline{\Delta}$  and  $\mathbf{c}$  defined in  
 676 Lemma B.3, we have

$$\mathbf{d} = \begin{bmatrix} -1 \\ -1 \end{bmatrix}, \bar{\Lambda} = \underline{\Lambda} = \begin{bmatrix} 0.9 & 0 \\ 0 & 0.8 \end{bmatrix}, \bar{\Delta} = \underline{\Delta} = 25, \mathbf{c} = -1, \quad (53)$$

677 from which and Equation (52), we then have

$$\bar{\mathbf{D}} = \frac{\mathbf{D}}{\bar{\Lambda}} = \underline{\mathbf{D}} = \frac{\mathbf{D}}{\underline{\Lambda}} = \begin{bmatrix} \frac{10}{9} & 0 & 0 & 0 \\ 0 & 0 & \frac{5}{4} & 0 \end{bmatrix}, \bar{\mathbf{C}} = \frac{\mathbf{C}}{\bar{\Delta}} = \underline{\mathbf{C}} = \frac{\mathbf{C}}{\underline{\Delta}} = \frac{1}{25}. \quad (54)$$

678 Then, for given  $\alpha = 0.87$ ,  $\beta = 0.002$ , and the model knowledge  $(\mathbf{A}, \mathbf{B})$  in [21], using the CVX  
 679 toolbox [53, 54], we obtain:

$$\mathbf{P} = \begin{bmatrix} 13.3812 & 6.9085 & 17.0004 & 3.6284 \\ 6.9085 & 4.1226 & 10.3597 & 2.2293 \\ 17.0004 & 10.3597 & 28.2701 & 5.8142 \\ 3.6284 & 2.2293 & 5.8142 & 1.2723 \end{bmatrix},$$

$$\mathbf{F} = \begin{bmatrix} 22.4008 & 16.9978 & 69.0659 & 12.6449 \end{bmatrix},$$

680 with which, physics model knowledge in Equation (51), and letting  $w(\mathbf{s}(k), \mathbf{a}(k)) = -\mathbf{a}_{\text{drl}}^2(k)$ , the  
 681 residual action policy 4 and the safety-embedded reward (5) are then ready for the Phy-DRL.

#### 682 F.4 HA-Teacher: Physics Knowledge and Design

683 Compared with HP-Student, HA-Teacher has relatively rich physics knowledge about system dynam-  
 684 ics, which is directly and equivalently transformed from Equation (49) as

$$\frac{d}{dt} \underbrace{\begin{bmatrix} x \\ \dot{x} \\ \theta \\ \dot{\theta} \end{bmatrix}}_{\mathbf{s}} = \underbrace{\begin{bmatrix} 0 & 1 & 0 & 0 \\ 0 & 0 & \frac{-m_p g \sin \theta \cos \theta}{\theta [\frac{4}{3}(m_c + m_p) - m_p \cos^2 \theta]} & \frac{\frac{4}{3} m_p l \sin \theta \dot{\theta}}{\frac{4}{3}(m_c + m_p) - m_p \cos^2 \theta} \\ 0 & 0 & 0 & 1 \\ 0 & 0 & \frac{g \sin \theta (m_c + m_p)}{l \theta [\frac{4}{3}(m_c + m_p) - m_p \cos^2 \theta]} & \frac{-m_p \sin \theta \cos \theta \dot{\theta}}{\frac{4}{3}(m_c + m_p) - m_p \cos^2 \theta} \end{bmatrix}}_{\hat{\mathbf{A}}(\mathbf{s})} \cdot \begin{bmatrix} x \\ \dot{x} \\ \theta \\ \dot{\theta} \end{bmatrix} + \underbrace{\begin{bmatrix} 0 \\ \frac{\frac{4}{3}}{\frac{4}{3}(m_c + m_p) - m_p \cos^2 \theta} \\ 0 \\ \frac{-\cos \theta}{l [\frac{4}{3}(m_c + m_p) - m_p \cos^2 \theta]} \end{bmatrix}}_{\hat{\mathbf{B}}(\mathbf{s})} \cdot \underbrace{\mathbf{F}}_{\mathbf{a}}, \quad (55)$$

685 where  $\hat{\mathbf{A}}(\mathbf{s})$  and  $\hat{\mathbf{B}}(\mathbf{s})$  are known to HA-Teacher. The sampling technique transforms the continuous-  
 686 time dynamics model (61) to the discrete-time one:

$$\mathbf{s}(k+1) = (\mathbf{I}_4 + T \cdot \hat{\mathbf{A}}(\mathbf{s})) \cdot \mathbf{s}(k) + T \cdot \hat{\mathbf{B}}(\mathbf{s}) \cdot \mathbf{a}(k),$$

687 from which we obtain the knowledge of  $\mathbf{A}(\bar{\mathbf{s}}^*)$  and  $\mathbf{B}(\bar{\mathbf{s}}^*)$  in Equation (11) as

$$\mathbf{A}(\bar{\mathbf{s}}^*) = \mathbf{I}_4 + T \cdot \hat{\mathbf{A}}(\bar{\mathbf{s}}^*) \text{ and } \mathbf{B}(\bar{\mathbf{s}}^*) = T \cdot \hat{\mathbf{B}}(\bar{\mathbf{s}}^*). \quad (56)$$

688 Meanwhile, for the center of the envelope patch (12), the model mismatch in Assumption 6.1, and the  
 689 switch-triggering condition and dwell time in (9), we let  $\chi = 0.25$ ,  $\kappa = 0.02$ ,  $\varepsilon = 0.6$ , and  $\tau = 10$ .  
 690 To always have feasible LMIs (17) and (18), we let  $\alpha = 0.95$  and  $\eta = 1.1$ . These parameters also  
 691 guarantee the condition in Equation (19) holds.

## 692 E.5 Additional Experimental Results

693 To further demonstrate the distinguished feature – lifetime safety, additional experimental results  
 694 are presented in Figure 7, Figure 8, and Figure 9, where the ‘Unsafe Continual Learning’ and ‘SeC-  
 695 Learning Machine’ are picked models trained after only **three episodes**, **four episodes**, **five episodes**,  
 respectively, in continual learning.

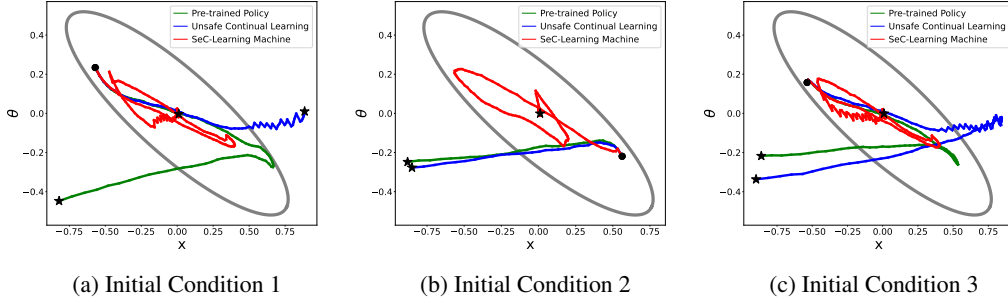


Figure 7: **Three Episodes**. Phase plots, given the same initial condition. The black dot and star denote the initial condition and final location, respectively.

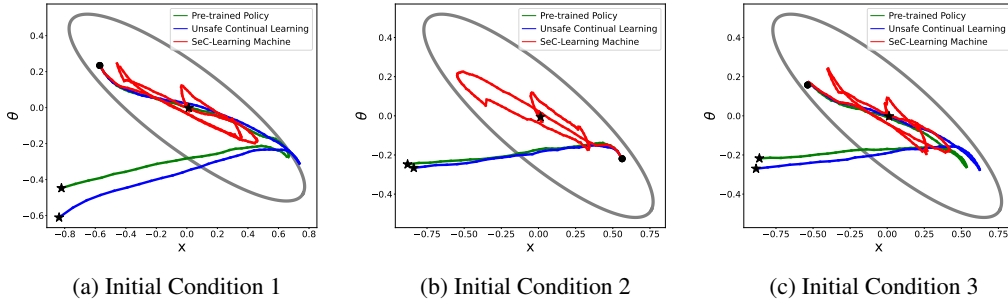


Figure 8: **Four Episodes** Phase plots, given the same initial condition. The black dot and star denote the initial condition and final location, respectively.

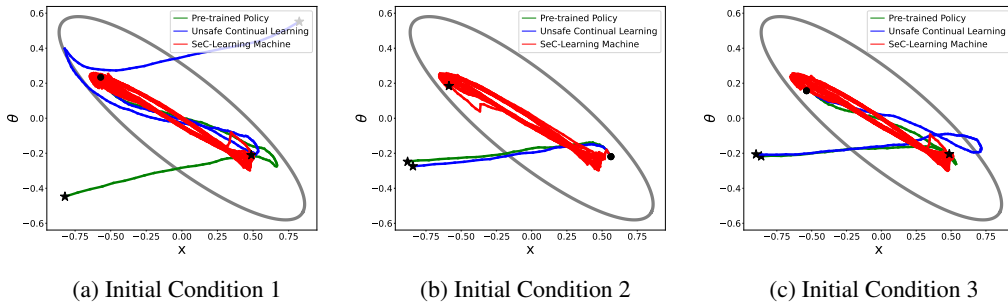


Figure 9: **Five Episodes**. Phase plots, given the same initial condition. The black dot and star denote the initial condition and final location, respectively.

696

## 697 G Experiment: Real Quadruped Robot

698 In the quadruped experiment, we adopt a Python-based framework for a Unitree A1 robot, released  
 699 in GitHub by [55]. The framework includes a simulation based on Pybullet, an interface for direct  
 700 sim-to-real transfer, and an implementation of the Convex MPC Controller for basic motion control.

### 701 G.1 Policy Learning

702 We train SeC-learning machine and Phy-DRL to achieve the safe mission introduced in Section 7.2.  
 703 The observation of the policy is a 12-dimensional tracking error vector between the robot’s state vector  
 704 and the mission vector. The agent’s actions offset the desired positional and lateral accelerations  
 705 generated from the model-based policy. The computed accelerations are then converted to the  
 706 low-level motors’ torque control.

707 The policy is trained using DDPG algorithm [41]. The actor and critic networks are implemented  
 708 as a Multi-Layer Perceptron (MLP) with four fully connected layers. The output dimensions of the  
 709 critic network are 256, 128, 64, and 1. The output dimensions of actor networks are 256, 128, 64, and  
 710 6. The input of the critic network is the tracking error vector and the action vector. The input of the  
 711 actor network is the tracking error vector. The activation functions of the first three neural layers are  
 712 ReLU, while the output of the last layer is the Tanh function for the actor network and Linear for  
 713 the critic network. In more detail, we let discount factor  $\gamma = 0.9$ , and the learning rates of critic and  
 714 actor networks are the same as 0.0003. We set the batch size to 512. The maximum step number for  
 715 one episode is 10,000.

### 716 G.2 System Dynamics

717 The physics knowledge about the robot used by HP-Student and HA-Teacher for their de-  
 718 signs is from the dynamics model of the robot, which is based on a single rigid body sub-  
 719 ject to forces at the contact patches [56]. The considered robot dynamics is characterized  
 720 by the position of the body’s center of mass (CoM) height  $h$ , the CoM velocity  $\mathbf{v} \triangleq \dot{\mathbf{p}} =$   
 721 [CoM x-velocity; CoM y-velocity; CoM z-velocity]  $\in \mathbb{R}^3$ , the Euler angles  $\tilde{\mathbf{e}} = [\phi; \theta; \psi] \in \mathbb{R}^3$   
 722 with  $\phi$ ,  $\theta$  and  $\psi$  being roll, pitch and yaw angles, respectively, and the angular velocity in world  
 723 coordinates  $\mathbf{w} \in \mathbb{R}^3$ .

724 According to the literature [56], the body dynamics of quadruped robots can be described by

$$\underbrace{\frac{d}{dt} \begin{bmatrix} h \\ \tilde{\mathbf{e}} \\ \mathbf{v} \\ \mathbf{w} \end{bmatrix}}_{\triangleq \hat{\mathbf{s}}} = \underbrace{\begin{bmatrix} \mathbf{O}_{1 \times 1} & \mathbf{O}_{1 \times 5} & 1 & \mathbf{O}_{1 \times 3} \\ \mathbf{O}_{3 \times 3} & \mathbf{O}_{3 \times 3} & \mathbf{O}_{3 \times 3} & \mathbf{R}(\phi, \theta, \psi) \\ \mathbf{O}_{3 \times 3} & \mathbf{O}_{3 \times 3} & \mathbf{O}_{3 \times 3} & \mathbf{O}_{3 \times 3} \\ \mathbf{O}_{3 \times 3} & \mathbf{O}_{3 \times 3} & \mathbf{O}_{3 \times 3} & \mathbf{O}_{3 \times 3} \end{bmatrix}}_{\triangleq \hat{\mathbf{A}}(\phi, \theta, \psi)} \cdot \begin{bmatrix} h \\ \tilde{\mathbf{e}} \\ \mathbf{v} \\ \mathbf{w} \end{bmatrix} + \hat{\mathbf{B}} \cdot \hat{\mathbf{a}} + \begin{bmatrix} 0 \\ \mathbf{O}_{3 \times 1} \\ \mathbf{O}_{3 \times 1} \\ \tilde{\mathbf{g}} \end{bmatrix} + \mathbf{f}(\hat{\mathbf{s}}), \quad (57)$$

725 where  $\tilde{\mathbf{g}} = [0; 0; -g] \in \mathbb{R}^3$  with  $g$  being the gravitational acceleration,  $\mathbf{f}(\hat{\mathbf{s}})$  denotes model mismatch,  
 726  $\hat{\mathbf{B}} = [\mathbf{O}_{4 \times 6}; \mathbf{I}_6]^\top$ , and the  $\mathbf{R}(\phi, \theta, \psi) = \mathbf{R}_z(\psi) \cdot \mathbf{R}_y(\theta) \cdot \mathbf{R}_x(\phi) \in \mathbb{R}^{3 \times 3}$  is the rotation matrix with

$$\mathbf{R}_x(\phi) = \begin{bmatrix} 1 & 0 & 0 \\ 0 & \cos \phi & -\sin \phi \\ 0 & \sin \phi & \cos \phi \end{bmatrix}, \mathbf{R}_y(\theta) = \begin{bmatrix} \cos \theta & 0 & \sin \theta \\ 0 & 1 & 0 \\ -\sin \theta & 0 & \cos \theta \end{bmatrix}, \mathbf{R}_z(\psi) = \begin{bmatrix} \cos \psi & -\sin \psi & 0 \\ \sin \psi & \cos \psi & 0 \\ 0 & 0 & 1 \end{bmatrix}.$$

### 727 G.3 HP-Student: Physics Knowledge and Design

728 To have the model knowledge represented by  $(\mathbf{A}, \mathbf{B})$  pertaining to robot dynamics (57), we make  
 729 the simplification:  $\mathbf{R}(\phi, \theta, \psi) = \mathbf{I}_3$ , which is obtained through setting the zero angels of roll, pitch  
 730 and yaw, i.e.,  $\phi = \theta = \psi = 0$ . Referring to (57) and ignoring unknown model mismatch, we can

731 obtain a simplified linear model pertaining to robot dynamics (57):

$$\underbrace{\frac{d}{dt} \begin{bmatrix} \tilde{h} \\ \tilde{e} \\ \tilde{v} \\ \tilde{w} \end{bmatrix}}_{\triangleq \tilde{s}} = \underbrace{\begin{bmatrix} \mathbf{O}_{1 \times 1} & \mathbf{O}_{1 \times 3} & 1 & \mathbf{O}_{1 \times 5} \\ \mathbf{O}_{3 \times 3} & \mathbf{O}_{3 \times 3} & \mathbf{O}_{3 \times 3} & \mathbf{R}(\phi, \theta, \psi) \\ \mathbf{O}_{3 \times 3} & \mathbf{O}_{3 \times 3} & \mathbf{O}_{3 \times 3} & \mathbf{O}_{3 \times 3} \\ \mathbf{O}_{3 \times 3} & \mathbf{O}_{3 \times 3} & \mathbf{O}_{3 \times 3} & \mathbf{O}_{3 \times 3} \end{bmatrix}}_{\triangleq \tilde{\mathbf{A}}} \cdot \begin{bmatrix} \tilde{h} \\ \tilde{e} \\ \tilde{v} \\ \tilde{w} \end{bmatrix} + \tilde{\mathbf{B}} \cdot \tilde{a} \quad (58)$$

732 Given the equilibrium point (or control goal)  $\mathbf{s}^*$  and  $\tilde{\mathbf{s}}$  given in Equation (58), we define  $\mathbf{s} \triangleq \tilde{\mathbf{s}} - \mathbf{s}^*$ .  
 733 It is then straightforward to obtain a dynamics from Equation (58) as  $\dot{\mathbf{s}} = \tilde{\mathbf{A}} \cdot \mathbf{s} + \tilde{\mathbf{B}} \cdot \tilde{\mathbf{a}}$ , which  
 734 transforms to a discrete-time model via sampling technique:

$$\mathbf{s}(k+1) = \mathbf{A} \cdot \mathbf{s}(k) + \mathbf{B} \cdot \tilde{\mathbf{a}}(k), \text{ with } \mathbf{A} = \mathbf{I}_{10} + T \cdot \tilde{\mathbf{A}} \text{ and } \mathbf{B} = T \cdot \tilde{\mathbf{B}}, \quad (59)$$

735 where  $T$  is the sampling period.

736 Considering the safety constraints in Section 7.2, we obtain the safety set defined in Equation (2),  
 737 where

$$\mathbf{D} = \begin{bmatrix} 0 & 0 & 0 & 1 & 0 & 0 & 0 & \mathbf{O}_{1 \times 3} \\ 1 & 0 & 0 & 0 & 0 & 0 & 0 & \mathbf{O}_{1 \times 3} \\ 0 & 0 & 0 & 0 & 1 & 0 & 0 & \mathbf{O}_{1 \times 3} \\ 0 & 0 & 0 & 0 & 0 & 0 & \mathbf{O}_{1 \times 3} & 1 \end{bmatrix}, \mathbf{v} = \begin{bmatrix} 0 \\ r_h \\ r_{v_x} \\ 0 \end{bmatrix}, \bar{\mathbf{v}} = \begin{bmatrix} 0.1 \\ 0.12 \\ |r_{v_x}| \\ 0.4 \end{bmatrix}, \underline{\mathbf{v}} = \begin{bmatrix} -0.1 \\ -0.12 \\ -|r_{v_x}| \\ -0.4 \end{bmatrix}, \quad (60)$$

738 Letting  $\alpha = 0.9$ , we obtain the following model-based solutions via LMI Solver in Matlab, which  
 739 satisfy the LMIs in Equation (24) and Equation (29).

$$\mathbf{P} = \begin{bmatrix} 122.1647861 & 0 & 0 & 0 & 2.487166 & 0 & 0 \\ 0 & 1.5e-06 & 0 & 0 & 0 & 0 & 0 \\ 0 & 0 & 1.5e-06 & 0 & 0 & 0 & 0 \\ 0 & 0 & 0 & 480.6210753 & 0 & 0 & 0 \\ 2.487166 & 0 & 0 & 0 & 3.2176033 & 0 & 0 \\ 0 & 0 & 0 & 0 & 0 & 1.3e-06 & 0 \\ 0 & 0 & 0 & 0 & 0 & 0 & 1.2e-06 \\ 0 & 9e-07 & 0 & 0 & 0 & 0 & 0 \\ 0 & 0 & 9e-07 & 0 & -0 & 0 & 0 \\ 0 & 0 & 0 & 155.2954559 & 0 & 0 & 0 \\ 0 & 0 & 0 & 0 & 0 & 0 & 0 \\ 9e-07 & 0 & 0 & 0 & 0 & 0 & 0 \\ 0 & 9e-07 & 0 & 0 & 0 & 0 & 0 \\ 0 & 0 & 155.2954559 & 0 & 0 & 0 & 0 \\ 0 & 0 & 0 & 0 & 0 & 0 & 0 \\ 0 & 0 & 0 & 0 & 0 & 0 & 0 \\ 7e-07 & 0 & 0 & 0 & 0 & 0 & 0 \\ 0 & 7e-07 & 0 & 0 & 0 & 0 & 0 \\ 0 & 0 & -0,156.3068079 & 0 & 0 & 0 & 0 \end{bmatrix},$$

$$\mathbf{F} = \begin{bmatrix} 0 & 0 & 0 & 0 & -23.65 & 0 & 0 & 0 & 0 & 0 \\ 0 & 0 & 0 & 0 & 0 & -20 & 0 & 0 & 0 & 0 \\ -63.11 & 0 & 0 & 0 & 0 & 0 & -20 & 0 & 0 & 0 \\ 0 & -32.51 & 0 & 0 & 0 & 0 & 0 & -21.88 & 0 & 0 \\ 0 & 0 & -32.51 & 0 & 0 & 0 & 0 & 0 & -21.88 & 0 \\ 0 & 0 & 0 & -30.95 & 0 & 0 & 0 & 0 & 0 & -22.28 \end{bmatrix},$$

740 with which and matrices  $\mathbf{A}$  and  $\mathbf{B}$  in Equation (59), we are able to deliver the residual action policy  
 741 (4) and safety-embedded reward (5).

#### 742 G.4 HA-Teacher: Physics Knowledge and Design

743 Compared with HP-Student, HA-Teacher has relatively rich physics knowledge about system dynam-  
 744 ics, which is directly and equivalently transformed from Equation (57) as

$$\frac{d}{dt} \underbrace{\begin{bmatrix} h \\ \tilde{\mathbf{e}} \\ \mathbf{v} \\ \mathbf{w} \end{bmatrix}}_{\mathbf{s}} = \underbrace{\begin{bmatrix} \mathbf{O}_{1 \times 1} & \mathbf{O}_{1 \times 3} & 1 & \mathbf{O}_{1 \times 5} \\ \mathbf{O}_{3 \times 3} & \mathbf{O}_{3 \times 3} & \mathbf{O}_{3 \times 3} & \mathbf{R}(\phi, \theta, \psi) \\ \mathbf{O}_{3 \times 3} & \mathbf{O}_{3 \times 3} & \mathbf{O}_{3 \times 3} & \mathbf{O}_{3 \times 3} \\ \mathbf{O}_{3 \times 3} & \mathbf{O}_{3 \times 3} & \mathbf{O}_{3 \times 3} & \mathbf{O}_{3 \times 3} \end{bmatrix}}_{\hat{\mathbf{A}}(\mathbf{s})} \cdot \underbrace{\begin{bmatrix} h \\ \tilde{\mathbf{e}} \\ \mathbf{v} \\ \mathbf{w} \end{bmatrix}}_{\mathbf{s}} + \underbrace{\begin{bmatrix} \mathbf{O}_3 & \mathbf{O}_3 & \mathbf{O}_3 & \mathbf{O}_3 \\ \mathbf{O}_3 & \mathbf{O}_3 & \mathbf{O}_3 & \mathbf{O}_3 \\ \mathbf{O}_3 & \mathbf{O}_3 & \mathbf{I}_3 & \mathbf{O}_3 \\ \mathbf{O}_3 & \mathbf{O}_3 & \mathbf{O}_3 & \mathbf{I}_3 \end{bmatrix}}_{\hat{\mathbf{B}}(\mathbf{s})} \cdot \mathbf{a} + \mathbf{g}(\mathbf{s}), \quad (61)$$

745 where  $\hat{\mathbf{A}}(\mathbf{s})$  and  $\hat{\mathbf{B}}(\mathbf{s})$  are known to HA-Teacher. The sampling technique transforms the continuous-  
 746 time dynamics model (61) to the discrete-time one:

$$\mathbf{s}(k+1) = (\mathbf{I}_4 + T \cdot \hat{\mathbf{A}}(\mathbf{s})) \cdot \mathbf{s}(k) + T \cdot \hat{\mathbf{B}}(\mathbf{s}) \cdot \mathbf{a}(k) + T \cdot \mathbf{g}(\mathbf{s}),$$

747 from which we obtain the knowledge of  $\mathbf{A}(\bar{\mathbf{s}}^*)$  and  $\mathbf{B}(\bar{\mathbf{s}}^*)$  in Equation (11) as

$$\mathbf{A}(\bar{\mathbf{s}}^*) = \mathbf{I}_4 + T \cdot \hat{\mathbf{A}}(\bar{\mathbf{s}}^*) \quad \text{and} \quad \mathbf{B}(\bar{\mathbf{s}}^*) = T \cdot \hat{\mathbf{B}}(\bar{\mathbf{s}}^*). \quad (62)$$

748 Meanwhile, for the center of the envelope patch (12), the model mismatch in Assumption 6.1, and the  
 749 switch-triggering condition and dwell time in (9), we let  $\chi = 0.25$ ,  $\kappa = 0.02$ ,  $\varepsilon = 0.6$ , and  $\tau = 10$ .  
 750 To always have feasible LMIs (17) and (18), we let  $\alpha = 0.99$  and  $\eta = 1.1$ . These parameters also  
 751 guarantee that the condition in Equation (19) is fulfilled.

#### 752 G.5 Additional Experimental Results

##### 753 G.5.1 Trajectories

754 The real robot's trajectories of COM height and COM x-velocities under the control of the SeC-  
 755 learning machine in the 5th episode, 10th episode, 15th episode, and 20th episode are shown in  
 756 Figures 10 to 13, respectively. The figures straightforwardly depict that the SeC-learning machine  
 757 guarantees the safety of real robots in all picked episodes of continual learning.

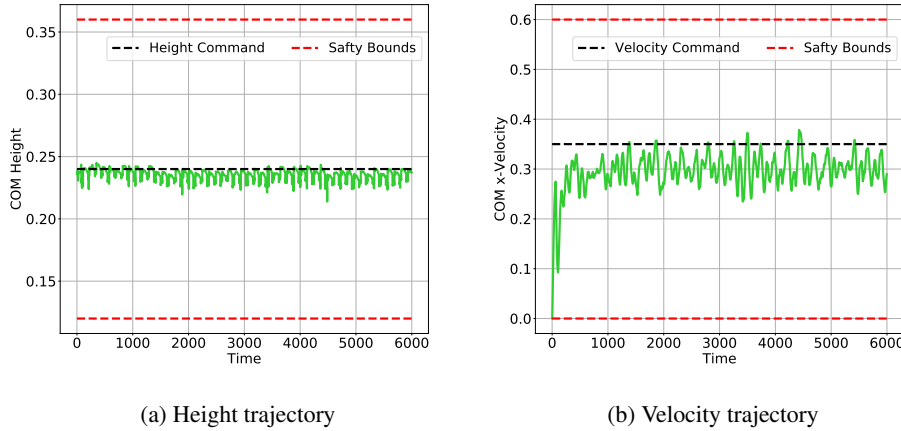
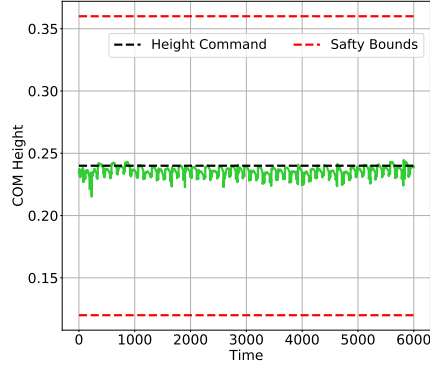


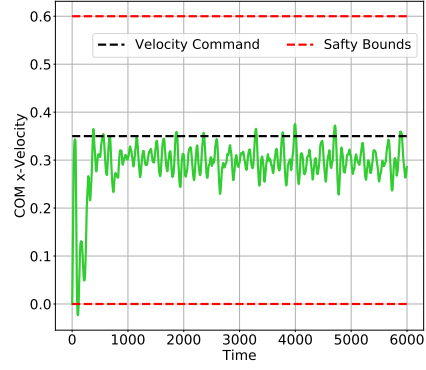
Figure 10: Robot's trajectories under control of SeC learning machine in the **5th Episode**.

##### 758 G.5.2 Reward

759 The reward curves in the iteration step for 20 episodes are shown in Figure 14. Observing Figure 14,  
 760 we conclude that given the same reward for learning, the SeC-Learning Machine exhibits remarkably  
 761 fast and stable learning, compared with continual learning without Simplex logic.

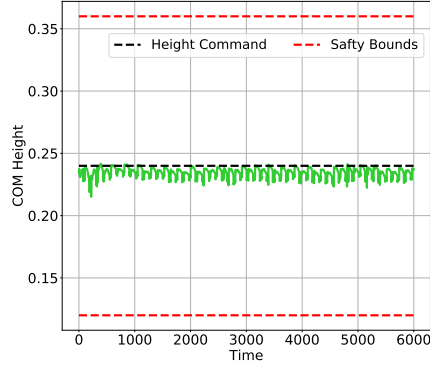


(a) Height trajectory

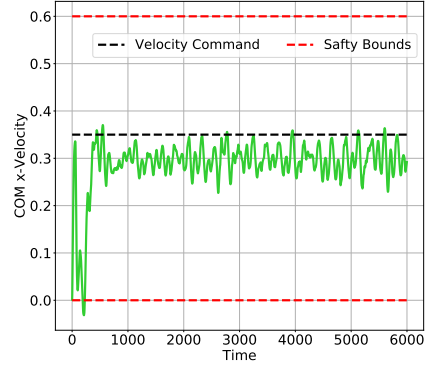


(b) Velocity trajectory

Figure 11: Robot's trajectories under control of SeC learning machine in the **10th Episode**.

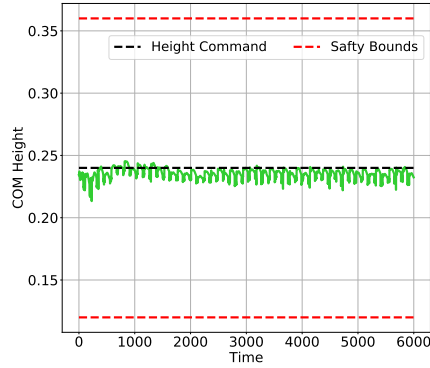


(a) Height trajectory



(b) Velocity trajectory

Figure 12: Robot's trajectories under control of SeC learning machine in the **15th Episode**.



(a) Height trajectory



(b) Velocity trajectory

Figure 13: Robot's trajectories under control of SeC learning machine in the **20th Episode**.

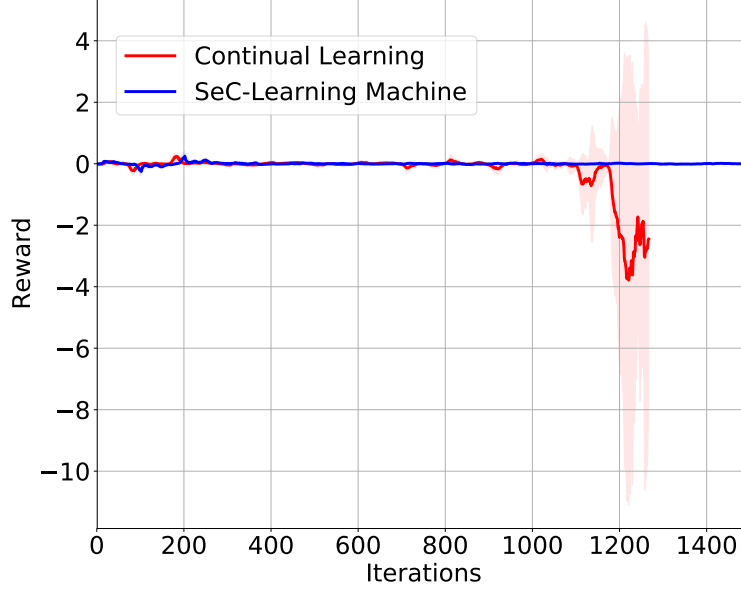


Figure 14: Reward curves in the term of iteration steps.

## 762 H Computation Resources

763 In all case studies, we train and test the deep reinforcement learning (DRL) algorithm on a desktop  
 764 equipped with Ubuntu 22.04, a 12th Gen Intel(R) Core(TM) i9-12900K 16-core processor, 64 GB of  
 765 RAM, and an NVIDIA GeForce GTX 3090 GPU. The DRL algorithm was implemented in Python  
 766 using the TensorFlow framework. We used the open-source Python CVX solver to solve LMIs  
 767 problems.

768 In our architecture, the computation of  $\hat{\mathbf{F}}$  and  $\hat{\mathbf{P}}$  for HA-Teacher at each patch need to be done  
 769 in time when the Safety Coordinator is triggered. To enable real-time computation of CVX and  
 770 interaction with the environment, we implement a multi-processing pipeline to control the robot and  
 771 solve LMIs in parallel in real-time. For solving LMIs, we always let the solver take the latest state so  
 772 that whenever the safety coordinator is triggered, the latest  $\hat{\mathbf{F}}$  and  $\hat{\mathbf{P}}$  will always be ready, where the  
 773 delay issue was considered and formulated in the LMIs problems.

774 We also noticed that the MATLAB-based CVX solver could solve the LMIs problem more consistently  
 775 than the Python-based one, yielding more reliable solutions. However, the data interfacing overhead  
 776 between Matlab and Python will introduce extra delay when updating  $\hat{\mathbf{F}}$  and  $\hat{\mathbf{P}}$  for HA-Teacher.  
 777 Besides, the multiprocessing implementation for Matlab and Python is another technical challenge  
 778 due to software compatibility issues. Therefore, we took the Python-based CVX solver for real-  
 779 time real-world experiments, and we suggest that the Matlab-based solver is preferable for the less  
 780 real-time sensitive applications.



## NeurIPS Paper Checklist

### 1. Claims

Question: Do the main claims made in the abstract and introduction accurately reflect the paper's contributions and scope?

Answer: [\[Yes\]](#)

Justification: See Section 1.3.

Guidelines:

- The answer NA means that the abstract and introduction do not include the claims made in the paper.
- The abstract and/or introduction should clearly state the claims made, including the contributions made in the paper and important assumptions and limitations. A No or NA answer to this question will not be perceived well by the reviewers.
- The claims made should match theoretical and experimental results, and reflect how much the results can be expected to generalize to other settings.
- It is fine to include aspirational goals as motivation as long as it is clear that these goals are not attained by the paper.

### 2. Limitations

Question: Does the paper discuss the limitations of the work performed by the authors?

Answer: [\[Yes\]](#)

Justification: See Section 8, and also Section 7 from experiment perspective.

Guidelines:

- The answer NA means that the paper has no limitation while the answer No means that the paper has limitations, but those are not discussed in the paper.
- The authors are encouraged to create a separate "Limitations" section in their paper.
- The paper should point out any strong assumptions and how robust the results are to violations of these assumptions (e.g., independence assumptions, noiseless settings, model well-specification, asymptotic approximations only holding locally). The authors should reflect on how these assumptions might be violated in practice and what the implications would be.
- The authors should reflect on the scope of the claims made, e.g., if the approach was only tested on a few datasets or with a few runs. In general, empirical results often depend on implicit assumptions, which should be articulated.
- The authors should reflect on the factors that influence the performance of the approach. For example, a facial recognition algorithm may perform poorly when image resolution is low or images are taken in low lighting. Or a speech-to-text system might not be used reliably to provide closed captions for online lectures because it fails to handle technical jargon.
- The authors should discuss the computational efficiency of the proposed algorithms and how they scale with dataset size.
- If applicable, the authors should discuss possible limitations of their approach to address problems of privacy and fairness.
- While the authors might fear that complete honesty about limitations might be used by reviewers as grounds for rejection, a worse outcome might be that reviewers discover limitations that aren't acknowledged in the paper. The authors should use their best judgment and recognize that individual actions in favor of transparency play an important role in developing norms that preserve the integrity of the community. Reviewers will be specifically instructed to not penalize honesty concerning limitations.

### 3. Theory Assumptions and Proofs

Question: For each theoretical result, does the paper provide the full set of assumptions and a complete (and correct) proof?

Answer: [\[Yes\]](#)

Justification: Assumption 6.1 formally states the assumption for HA-Teacher design.

Guidelines:

- The answer NA means that the paper does not include theoretical results.
- All the theorems, formulas, and proofs in the paper should be numbered and cross-referenced.
- All assumptions should be clearly stated or referenced in the statement of any theorems.
- The proofs can either appear in the main paper or the supplemental material, but if they appear in the supplemental material, the authors are encouraged to provide a short proof sketch to provide intuition.
- Inversely, any informal proof provided in the core of the paper should be complemented by formal proofs provided in appendix or supplemental material.
- Theorems and Lemmas that the proof relies upon should be properly referenced.

#### 4. Experimental Result Reproducibility

Question: Does the paper fully disclose all the information needed to reproduce the main experimental results of the paper to the extent that it affects the main claims and/or conclusions of the paper (regardless of whether the code and data are provided or not)?

Answer: [Yes]

Justification: The paper has disclosed all the information needed to reproduce the paper's main results, see Appendices F.3, F.4, G.3 and G.4 for (design) details of experiments.

Guidelines:

- The answer NA means that the paper does not include experiments.
- If the paper includes experiments, a No answer to this question will not be perceived well by the reviewers: Making the paper reproducible is important, regardless of whether the code and data are provided or not.
- If the contribution is a dataset and/or model, the authors should describe the steps taken to make their results reproducible or verifiable.
- Depending on the contribution, reproducibility can be accomplished in various ways. For example, if the contribution is a novel architecture, describing the architecture fully might suffice, or if the contribution is a specific model and empirical evaluation, it may be necessary to either make it possible for others to replicate the model with the same dataset, or provide access to the model. In general, releasing code and data is often one good way to accomplish this, but reproducibility can also be provided via detailed instructions for how to replicate the results, access to a hosted model (e.g., in the case of a large language model), releasing of a model checkpoint, or other means that are appropriate to the research performed.
- While NeurIPS does not require releasing code, the conference does require all submissions to provide some reasonable avenue for reproducibility, which may depend on the nature of the contribution. For example
  - (a) If the contribution is primarily a new algorithm, the paper should make it clear how to reproduce that algorithm.
  - (b) If the contribution is primarily a new model architecture, the paper should describe the architecture clearly and fully.
  - (c) If the contribution is a new model (e.g., a large language model), then there should either be a way to access this model for reproducing the results or a way to reproduce the model (e.g., with an open-source dataset or instructions for how to construct the dataset).
  - (d) We recognize that reproducibility may be tricky in some cases, in which case authors are welcome to describe the particular way they provide for reproducibility. In the case of closed-source models, it may be that access to the model is limited in some way (e.g., to registered users), but it should be possible for other researchers to have some path to reproducing or verifying the results.

#### 5. Open access to data and code

Question: Does the paper provide open access to the data and code, with sufficient instructions to faithfully reproduce the main experimental results, as described in supplemental material?

Answer: [Yes]

Justification: The paper has disclosed all the information needed to reproduce the paper's main results. The source code has been submitted as supplemental material and will be disclosed to the public via GitHub.

Guidelines:

- The answer NA means that paper does not include experiments requiring code.
- Please see the NeurIPS code and data submission guidelines (<https://nips.cc/public/guides/CodeSubmissionPolicy>) for more details.
- While we encourage the release of code and data, we understand that this might not be possible, so "No" is an acceptable answer. Papers cannot be rejected simply for not including code, unless this is central to the contribution (e.g., for a new open-source benchmark).
- The instructions should contain the exact command and environment needed to run to reproduce the results. See the NeurIPS code and data submission guidelines (<https://nips.cc/public/guides/CodeSubmissionPolicy>) for more details.
- The authors should provide instructions on data access and preparation, including how to access the raw data, preprocessed data, intermediate data, and generated data, etc.
- The authors should provide scripts to reproduce all experimental results for the new proposed method and baselines. If only a subset of experiments are reproducible, they should state which ones are omitted from the script and why.
- At submission time, to preserve anonymity, the authors should release anonymized versions (if applicable).
- Providing as much information as possible in supplemental material (appended to the paper) is recommended, but including URLs to data and code is permitted.

## 6. Experimental Setting/Details

Question: Does the paper specify all the training and test details (e.g., data splits, hyperparameters, how they were chosen, type of optimizer, etc.) necessary to understand the results?

Answer: [Yes]

Justification: See Appendices F.1 and G.1 for details.

Guidelines:

- The answer NA means that the paper does not include experiments.
- The experimental setting should be presented in the core of the paper to a level of detail that is necessary to appreciate the results and make sense of them.
- The full details can be provided either with the code, in appendix, or as supplemental material.

## 7. Experiment Statistical Significance

Question: Does the paper report error bars suitably and correctly defined or other appropriate information about the statistical significance of the experiments?

Answer: [Yes]

Justification: See statistical result in Figure 4.

Guidelines:

- The answer NA means that the paper does not include experiments.
- The authors should answer "Yes" if the results are accompanied by error bars, confidence intervals, or statistical significance tests, at least for the experiments that support the main claims of the paper.
- The factors of variability that the error bars are capturing should be clearly stated (for example, train/test split, initialization, random drawing of some parameter, or overall run with given experimental conditions).
- The method for calculating the error bars should be explained (closed form formula, call to a library function, bootstrap, etc.)
- The assumptions made should be given (e.g., Normally distributed errors).

- It should be clear whether the error bar is the standard deviation or the standard error of the mean.
- It is OK to report 1-sigma error bars, but one should state it. The authors should preferably report a 2-sigma error bar than state that they have a 96% CI, if the hypothesis of Normality of errors is not verified.
- For asymmetric distributions, the authors should be careful not to show in tables or figures symmetric error bars that would yield results that are out of range (e.g. negative error rates).
- If error bars are reported in tables or plots, The authors should explain in the text how they were calculated and reference the corresponding figures or tables in the text.

## 8. Experiments Compute Resources

Question: For each experiment, does the paper provide sufficient information on the computer resources (type of compute workers, memory, time of execution) needed to reproduce the experiments?

Answer: [Yes]

Justification: See Appendix H for details.

Guidelines:

- The answer NA means that the paper does not include experiments.
- The paper should indicate the type of compute workers CPU or GPU, internal cluster, or cloud provider, including relevant memory and storage.
- The paper should provide the amount of compute required for each of the individual experimental runs as well as estimate the total compute.
- The paper should disclose whether the full research project required more compute than the experiments reported in the paper (e.g., preliminary or failed experiments that didn't make it into the paper).

## 9. Code Of Ethics

Question: Does the research conducted in the paper conform, in every respect, with the NeurIPS Code of Ethics <https://neurips.cc/public/EthicsGuidelines>?

Answer: [Yes]

Justification: Completely conform with the NeurIPS Code of Ethics!

Guidelines:

- The answer NA means that the authors have not reviewed the NeurIPS Code of Ethics.
- If the authors answer No, they should explain the special circumstances that require a deviation from the Code of Ethics.
- The authors should make sure to preserve anonymity (e.g., if there is a special consideration due to laws or regulations in their jurisdiction).

## 10. Broader Impacts

Question: Does the paper discuss both potential positive societal impacts and negative societal impacts of the work performed?

Answer: [NA]

Justification: This paper has no such issues, as it does not involve human subjects, animals, privacy, or social security.

Guidelines:

- The answer NA means that there is no societal impact of the work performed.
- If the authors answer NA or No, they should explain why their work has no societal impact or why the paper does not address societal impact.
- Examples of negative societal impacts include potential malicious or unintended uses (e.g., disinformation, generating fake profiles, surveillance), fairness considerations (e.g., deployment of technologies that could make decisions that unfairly impact specific groups), privacy considerations, and security considerations.

- The conference expects that many papers will be foundational research and not tied to particular applications, let alone deployments. However, if there is a direct path to any negative applications, the authors should point it out. For example, it is legitimate to point out that an improvement in the quality of generative models could be used to generate deepfakes for disinformation. On the other hand, it is not needed to point out that a generic algorithm for optimizing neural networks could enable people to train models that generate Deepfakes faster.
- The authors should consider possible harms that could arise when the technology is being used as intended and functioning correctly, harms that could arise when the technology is being used as intended but gives incorrect results, and harms following from (intentional or unintentional) misuse of the technology.
- If there are negative societal impacts, the authors could also discuss possible mitigation strategies (e.g., gated release of models, providing defenses in addition to attacks, mechanisms for monitoring misuse, mechanisms to monitor how a system learns from feedback over time, improving the efficiency and accessibility of ML).

## 11. Safeguards

Question: Does the paper describe safeguards that have been put in place for responsible release of data or models that have a high risk for misuse (e.g., pretrained language models, image generators, or scraped datasets)?

Answer: [NA]

Justification: The paper poses no such risks, as the application domain is the learning-enabled autonomous systems, and the ‘models’ we are using are the well-validated physics-dynamics models.

Guidelines:

- The answer NA means that the paper poses no such risks.
- Released models that have a high risk for misuse or dual-use should be released with necessary safeguards to allow for controlled use of the model, for example by requiring that users adhere to usage guidelines or restrictions to access the model or implementing safety filters.
- Datasets that have been scraped from the Internet could pose safety risks. The authors should describe how they avoided releasing unsafe images.
- We recognize that providing effective safeguards is challenging, and many papers do not require this, but we encourage authors to take this into account and make a best faith effort.

## 12. Licenses for existing assets

Question: Are the creators or original owners of assets (e.g., code, data, models) used in the paper properly credited, and are the license and terms of use explicitly mentioned and properly respected?

Answer: [Yes]

Justification: The paper cites all the building blocks. Specifically, the developed Sec-learning machine is built on DDPG [41], Phy-DRL [21, 22], and Simplex [36, 37]. The experiments on cart-pole system are performed on Open-AI Gym [48]. In the quadruped robot experiment, we adopt a Python-based framework for a Unitree A1 robot, released in GitHub in [55].

Guidelines:

- The answer NA means that the paper does not use existing assets.
- The authors should cite the original paper that produced the code package or dataset.
- The authors should state which version of the asset is used and, if possible, include a URL.
- The name of the license (e.g., CC-BY 4.0) should be included for each asset.
- For scraped data from a particular source (e.g., website), the copyright and terms of service of that source should be provided.

- If assets are released, the license, copyright information, and terms of use in the package should be provided. For popular datasets, [paperswithcode.com/datasets](https://paperswithcode.com/datasets) has curated licenses for some datasets. Their licensing guide can help determine the license of a dataset.
- For existing datasets that are re-packaged, both the original license and the license of the derived asset (if it has changed) should be provided.
- If this information is not available online, the authors are encouraged to reach out to the asset's creators.

### 13. New Assets

Question: Are new assets introduced in the paper well documented and is the documentation provided alongside the assets?

Answer: [\[Yes\]](#)

Justification: All new assets are well documented and submitted as supplemental material.

Guidelines:

- The answer NA means that the paper does not release new assets.
- Researchers should communicate the details of the dataset/code/model as part of their submissions via structured templates. This includes details about training, license, limitations, etc.
- The paper should discuss whether and how consent was obtained from people whose asset is used.
- At submission time, remember to anonymize your assets (if applicable). You can either create an anonymized URL or include an anonymized zip file.

### 14. Crowdsourcing and Research with Human Subjects

Question: For crowdsourcing experiments and research with human subjects, does the paper include the full text of instructions given to participants and screenshots, if applicable, as well as details about compensation (if any)?

Answer: [\[NA\]](#) .

Justification: This paper does not involve human subjects and animals. The applications are the safety-critical learning-enabled autonomous systems.

Guidelines:

- The answer NA means that the paper does not involve crowdsourcing nor research with human subjects.
- Including this information in the supplemental material is fine, but if the main contribution of the paper involves human subjects, then as much detail as possible should be included in the main paper.
- According to the NeurIPS Code of Ethics, workers involved in data collection, curation, or other labor should be paid at least the minimum wage in the country of the data collector.

### 15. Institutional Review Board (IRB) Approvals or Equivalent for Research with Human Subjects

Question: Does the paper describe potential risks incurred by study participants, whether such risks were disclosed to the subjects, and whether Institutional Review Board (IRB) approvals (or an equivalent approval/review based on the requirements of your country or institution) were obtained?

Answer: [\[NA\]](#)

Justification: This paper does not involve human subjects and animals. The applications are the safety-critical learning-enabled autonomous systems.

Guidelines:

- The answer NA means that the paper does not involve crowdsourcing nor research with human subjects.

- 1091 • Depending on the country in which research is conducted, IRB approval (or equivalent)  
1092 may be required for any human subjects research. If you obtained IRB approval, you  
1093 should clearly state this in the paper.
- 1094 • We recognize that the procedures for this may vary significantly between institutions  
1095 and locations, and we expect authors to adhere to the NeurIPS Code of Ethics and the  
1096 guidelines for their institution.
- 1097 • For initial submissions, do not include any information that would break anonymity (if  
1098 applicable), such as the institution conducting the review.